AMERICAN UNIVERSITY OF BEIRUT

NEAR OPTIMAL CONTROL OF HYBRID FUEL CELL ELECTRIC VEHICLE IN REAL-TIME

by
CARLA ALI MAJED

A thesis
submitted in partial fulfillment of the requirements
for the degree of Master of Engineering
to the Department of Electrical and Computer Engineering
of the Faculty of Engineering and Architecture
at the American University of Beirut

Beirut, Lebanon
September 2015

AMERICAN UNIVERSITY OF BEIRUT

NEAR OPTIMAL CONTROL OF HYBRID FUEL CELL
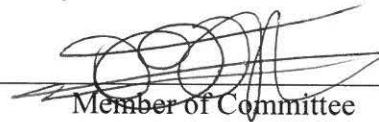ELECTRIC VEHICLE IN REAL-TIME

by
CARLA ALI MAJED

Approved by:

_____

Dr. Sami Karaki, Professor   Advisor
Electrical and Computer Engineering

_____

Dr. Rabih Jabr, Professor   Member of Committee
Electrical and Computer Engineering

_____

Dr. Mariette Awad, Associate Professor   Member of Committee
Electrical and Computer Engineering

Date of thesis/dissertation defense: [Sept 14, 2015]

AMERICAN UNIVERSITY OF BEIRUT

THESIS, DISSERTATION, PROJECT RELEASE FORM

Student Name:
___Majed_____Carla_____Ali___
              Last   First   Middle

⊘ Master's Thesis   ◯ Master's Project   ◯ Doctoral Dissertation

☑ I authorize the American University of Beirut to: (a) reproduce hard or electronic copies of my thesis, dissertation, or project; (b) include such copies in the archives and digital repositories of the University; and (c) make freely available such copies to third parties for research or educational purposes.

☐ I authorize the American University of Beirut, **three years after the date of submitting my thesis, dissertation, or project,** to: (a) reproduce hard or electronic copies of it; (b) include such copies in the archives and digital repositories of the University; and (c) make freely available such copies to third parties for research or educational purposes.

_____   Sept. 29th, 2015
Signature   Date

ACKNOWLEDGMENTS

I would like to express my sincere gratitude to all those people who have supported me and had their contribution in making this thesis possible.

I would like to express my deep gratitude to my advisor Prof. Sami Karaki for his supervision, advice, guidance, and help through the leaning process of this thesis. I have been extremely lucky to have a supervisor who cared so much about my work, and who responded to my questions so promptly

I am also grateful to other committee members, Prof. Rabih Jabr and Prof. Mariette Awad for their valuable advices and comments during the achievement of this thesis.

I would like to thank the American University of Beirut, the Electrical and Computer Engineering Department, and particularly Mrs. Rabab Abi Shakra for all their help and support during the two years of my master's journey. I am really proud to be a member of the AUB community.

I would also like to thank my family (Mom, Dad and brother) who believed in me and sacrificed so much in order to get to what I have reached today. I would also like to thank my fiancé for supporting me during the achievement of this thesis and for always being there for me.

I dedicate this thesis to my beloved country Lebanon.

AN ABSTRACT OF THE THESIS OF

Carla Ali Majed   for   Master of Electrical and Computer Engineering
                                 Major: Energy and Power Systems

Title: Near Optimal Control of Hybrid Fuel Cell Electric Vehicles in Real-Time

Hybrid electric vehicles (HEV) improvements in fuel economy and emissions strongly depend on the energy management strategy used whose aim is to minimize the hydrogen and battery cost. In this work a new control strategy called single step dynamic programming optimization (SSDP) and an energy management system based on artificial neural network are presented. These real-time energy management systems for HEV are derived from a dynamic programming (DP) technique. The DP requires that a forecast of the car torque requirement over the whole trip or part of it is available. However, in real time the road and driving conditions are not known a priori. The methods presented in this work can easily lend themselves for real time implementation. The problem formulation accounts for the power balance at each stage, the power limits, the state-of-charge (SOC) limits, and the ramp rates constraints of the fuel cell and battery. The SSDP optimization technique differs from DP in that it is a forward-looking model in which the controller makes instantaneous decisions without the need for back-tracing; therefore, it is more realistic than backward-looking models. It requires that only the demand at the next period should be known a priori and not the whole road. The proposed ANN is trained based on DP results carried out off-line. It can be implemented in real time as it takes one step at a time. The results obtained using both methods show that the fuel economy that can be achieved is very close to optimal results. Moreover, the two proposed methods provide an easy mechanism to change from charge sustaining (CS) to charge depleting (CD) operation simply by changing the lower bound of the battery SOC. To solve the SSDP and the ANN methods the demand at the next step should be known a priori. This demand is obtained by applying a one step-ahead speed forecast. The model used is a first order linear model also known as persistence forecast; it does not require an adaptive mechanism to adapt to changes in road conditions in real time. When the forecasted speed which is shifted from the actual speed by one step is used with SSDP, the fuel economy results obtained are very close to optimal ones obtained by DP. Verification of the methodologies is provided by comparing their results to those obtained by DP. Results on practical vehicle designs proposed in the literature are presented for the UDDS, HWFET, and NEDC standard driving cycles.

CONTENTS

ILLUSTRATIONS

x

TABLES

ABBREVIATIONS

HEV: Hybrid electric vehicle

DP: Dynamic program

SSDP: Single step dynamic program

ANN: Artificial neural network

CS: Charge sustaining

CD: Charge depleting

SOC: State of charge

UDDS: Urban dynamometer drive cycle

HWFET: Highway fuel economy test

NEDC: New European drive cycle

GHG: Greenhouse gases

FCHEV: Fuel cell hybrid electric vehicle

ICE: Internal combustion engine

PEMFC: Polymer electrolyte membrane fuel cell

FIS: Fuzzy inference system

EMS: Energy management system

UC: Ultra capacitor

FC: Fuel cell

PMP: Pontryagin Minimum Principle

RB: Rule base

ECMS: Equivalent consumption minimization strategy

PWM: Pulse width modulated

FDP: Forward dynamic program

TDP: Tunnel dynamic program

ABR: All battery range

CHAPTER I

INTRODUCTION

In the wake of the Kyoto protocol (1997) -an international treaty on global warming- attention has shifted towards new technology issues such as energy conservation, energy efficiency, and renewable energy as prospective solutions to global warming and measures to reduce the dependence on exhaustible fossil fuels. According to the International Energy Agency, primary energy consumption has increased by 49% during the last two decades (1984-2004) accompanied by an increase in CO_2 emissions in the atmosphere by 43% [1]. This has created a great research interest in alternative energy resources in the transport sector, a major contributor to greenhouse gases (GHG) emissions. The fuel cell hybrid electric vehicle (FCHEV) appears to be a possible solution to replace the internal combustion engine (ICE) in vehicular applications when the overall economics are favorable and the hydrogen refueling technology and infrastructure become available. Hybrid electric vehicles compared to conventional internal combustion engine can substantially reduce fuel consumption and hence pollution emissions, due to the possibility of downsizing the engine, the use of regenerative braking [14], the ability to satisfy the demand either from the battery or the fuel cell, and because hydrogen can be obtained from renewable resources. Therefore, FCHEV can lead to clean and efficient load transportation since it plays a vital role in increasing energy conversion efficiency and reducing exhaust emissions.

1

The FCHEV has two energy sources that drive the wheels; the primary source is a polymer electrolyte membrane fuel cell (PEMFC) that converts hydrogen and oxygen into electric energy and produces water and heat as by products. The secondary source is an energy storage system, which can be a battery that is either charged or discharged depending on the operating conditions of the vehicle. The output power delivered to the wheels may come from the battery or the fuel cell; therefore a control strategy is needed to determine at any time the power split between the two sources.

The power split problem should be solved optimally with the aim to reduce the operating cost made-up of hydrogen fuel consumption and battery degradation without compromising the driving comfort. This is the basis of energy efficiency in which unnecessary energy is reduced without affecting individual welfare. Some authors have proposed optimal control strategies to minimize the operating cost of the vehicle; others have adopted approaches that lend themselves more readily to real time implementation.

A. Literature Review

Some global optimization algorithms such as dynamic programming (DP) have been proposed in literature. Karaki et al. [2] describe the development of an optimizing energy management system based on dynamic programming to manage the fuel cell and battery outputs with the aim to reduce the hydrogen consumption by the fuel cell. The method is able to produce optimum results but it cannot be implemented in real-time since it requires speed forecast of the whole drive cycle. Schell et al. [3] describe the use of stochastic dynamic programming in vehicle design and model-based control algorithms to make it possible to increase fuel economy by 2–3% (an increase of about 15 km in range).

Perez et al. [4] use DP to determine the optimal split between sources for off-line use, for the hybrid electric vehicle (HEV) design, and for component sizing. They note that it may be used for on-line purposes by considering short term horizons, assuming that the driving schedule will not change dramatically. It seems that DP is the perfect tool for optimal control of HEV in the sense that it solves the problem and finds optimal solution and it can be used as a basis of comparison for evaluating other control strategies. However, the results obtained are not suitable for real time conditions since the problem must be known and well formulated for all its duration. In other words, the driving schedule over which the fuel consumption is minimized must be entirely known at the beginning of the trip which is not the case in real time. Therefore, it is imperative to develop a real time control strategy which does not depend on a priori knowledge to determine the best power split with a good overall performance. The solution will necessarily be suboptimal but can be implemented in real time.

Some authors use supervised learning such as neural networks and fuzzy inference systems (FIS) to develop a real time control strategy. The output of these systems constitutes an approximate optimal control strategy of the problem. Boyali and Guvens [5] use DP to generate the optimal pattern of control and then use supervised learning to train an artificial neural network (ANN) to approximate the pattern obtained by DP. The approximate results of the ANN are close to the optimum ones obtained from the DP method. Feldkamp et al. [6] use an ultra-capacitor as a secondary source in the HEV and propose a method based on ANN to do the power split. The inputs of the ANN are the vehicle speed, power at the wheels, and the ultra-capacitor state of charge, whereas the output is the power split. During training a stochastic perturbation is added to the data. The

3

ANN proved to be robust since it is able to produce near optimal results with different drive cycles. Yi et al. [7] propose a control strategy based on identifying driving cycles using fuzzy neural network in order to optimize the parameters of the control strategy which reduce the fuel consumption and emissions of the HEV. Lin and Zheng [8] formulate energy management as a constrained optimal control problem and use the penalty-function method to transform the problem into an unconstrained one. Supervised learning is then used to produce a neural network whose output constitutes an approximate optimal control strategy of the problem. Quigley et al. [9] propose a fuzzy clustering approach with single input (departure time) or dual input (departure time and vehicle use) to obtain journey parameters (distance and duration) needed to manage the energy flow through HEV. Single and dual FIS performed well for distance prediction; however, the dual system improved the FIS for distance prediction and worsens it for duration prediction. The system is able to generalize and perform well on new unseen examples. Xiong et al. [10] describe an energy management system that governs the series-parallel mode post-transmission switching as well as the instantaneous power distribution in a hybrid bus using two separate fuzzy logic controllers. The energy consumption is theoretically reduced by about 30% to that of the conventional bus under transit bus driving cycle. Erdinc et al. [11] describe an energy management system (EMS) based on fuzzy logic and wavelet transform to control power distribution in a hybrid PEMFC-Battery-ultra-capacitor (UC) vehicular system. Simulation shows that the SOC value of both battery and UC can be maintained within suitable limits. Accordingly this causes the fuel cell (FC) system to operate in its linear region, which is most efficient, thus leading to a decrease in the size of FC system and its fuel consumption.

The difficulty of implementing optimal control strategies in real time driving conditions led researchers to tackle the energy management problem using a rule based approach. Kim and Rousseau [12] compare two control strategies that are used to minimize fuel consumption in HEV. The first is rule-based and the second is based on instantaneous optimization that minimizes the system losses at every sample time. The instantaneous optimization is applied using linear quadratic regulator that calculates the optimal torque. The results obtained are compared to global optimal ones obtained from a Pontryagin Minimum Principle (PMP)-based optimal control. The optimal system is controlled by a co-state needed to bring the SOC to an appropriate final value. This co-state is selected by introducing an adaptive mechanism. The instantaneous optimal control produces similar fuel economies to global optimal solution than does the rule-based; it is also faster and does not require tuning by engineers. Ambuhl et al. [13] show that the explicit solution of the optimal control problem, of a simplified speed-independent unconstrained model, can be expressed as a simple rule-based map where all regions are defined by model parameters. The benefit of this formulation is the simple structure and the low number of possible minima. Simulations show that the maximum error is 1.6% in the final state and 1.0% in the final cost for three commonly used driving cycles. Sorrentino et al. [14] carried out a performance assessment of a rule-based (RB) control strategy for real time energy management of series HEV power-trains. Simulations were conducted on driving cycles of differing features to investigate the dependence of power prediction on the RB strategy used. The potential for on-board implementation of the RB control strategy were analyzed by coupling the heuristic rules with a-posteriori estimation of average traction power. Rule based methods to schedule the fuel cell and battery power levels have been used by Panik

et al. [15]. When the load torque is positive, the controller will try to satisfy this load from the fuel cell or the battery depending on the H_2 level in the tank and the state-of-charge (SOC) of the battery. One important operating mode is when the torque load is negative; in this case the mechanical drive train system is supplying power to the dc bus obtained by regenerative braking from the kinetic energy of the car when it is slowing down or when the car is going downhill.

Some authors propose a real time control strategy based on instantaneous optimization which requires the minimization of the cost function at each instant. The cost function depends on the fuel consumption and battery state of charge (SOC). Different approaches have been used to include the SOC in the cost function, a promising approach called Equivalent Consumption Minimization Strategy (ECMS) which is relatively faster than other strategies proposed in literature have been investigated. It consists of evaluating the instantaneous cost function as a sum of fuel consumption and equivalent fuel consumption representing the SOC. The optimality of the ECMS method is sensitive to the equivalent factor values that are based on the knowledge of the whole driving cycle. To make ECMS feasible for online operations, Mussardo et al. [16] use Kalman filter to predict future values of the vehicle speed and the optimal equivalence factor has been found by online optimization over a receding horizon. The method gives good results but is computationally demanding. Onori et al. [17] use a feedback controller applied at regular intervals of duration to update the value of the equivalence factor to account for the deviation of the SOC from its reference value. The proposed method is implementable in real time at low computational burden and is able to achieve results close to optimal global solution obtained from DP. Sciarretta et al. [18] present a control of the ECMS strategy. It

is based on a new method for evaluating the equivalence factor which does not require the assumption of the average efficiencies of the parallel paths. The fuel equivalent is calculated online as a function of the current system status and, in particular, of quantities that are measurable on board. Therefore, no predictions are needed for the future, and only few control parameters are required. The results illustrate the potential of the proposed method in terms of reducing fuel consumption and maintaining SOC sustainability. Rousseau et al. [19] present a study focused on variations of the size of power train components and optimization of the power split between engine and electric motor. They have implemented a DP over NEDC under constraints on battery SOC to obtain the optimal power split at each time step. Since DP cannot be implemented in real time, they have applied ECMS inferred from Pontryagin Minimum Principle (PMP), where they have chosen an average value for the price of electric energy estimated from offline optimization results. The fuel consumption obtained with ECMS is 326.8g compared to 310.34g obtained with DP using Matlab model. Gurkaynak et al. [20] propose a control strategy for HEV using the equivalent consumption minimization strategy (ECMS). In this study, a neural network is proposed to recognize driving cycles in an attempt to reduce the algorithm's sensitivity to variations in the drive cycle which allow the implementation of such models in real-time rendering them more "implementable". The obtained results are close to optimal ones of the dynamic programming.

Other methods used in literature for the optimization of resources in a FCHEV include Pontryagin Minimum Principle (PMP) which is a global optimization technique like DP, linear programming, lookup table, and predictive scheme. Bernard et al. [21] propose a real-time control, charge-sustaining, strategy for fuel cell hybrid vehicles, which

is derived from a non-causal algorithm based on the Pontryagin Minimum Principle (PMP). The control strategy is validated experimentally using a hardware-in-the-loop test bench. Serrao et al. [22] have considered new issues for the energy management of HEV to include more complete and complex cases that are solved using PMP. They have added new optimization criteria that extend beyond fuel consumption minimization to deal with emissions and battery aging simply by modifying the cost function. These applications are simple, immediate, and yield good results. They have also considered cases with additional states such as engine and catalyst temperature or battery temperature in which they have provided the basis for an analytical solution. Dinnawi et al. [23] use a linear programming technique to control the energy flow in a HEV considering several constrains. The proposed method is tested over the HWFET and UDDS drive cycles. It is able to produce optimum power split results capable of reducing hydrogen consumption and operation cost. Wang and Lukic [24] applied DP to series and parallel drive trains and investigated fuel economy and battery health. They developed a lookup table for real time control based on the DP approach and report improvements of the order of 27% of overall cost. Johanesson et al. [25] propose a predictive scheme that uses information from GPS and data record of the driving along the bus route to schedule the charging and discharging of the energy storage system. The scheme results in improved control of the SOC and the switching between hybrid and pure electric mode. The predictive scheme can be implemented in real time since the majority of the calculations are moved outside the real time loop, reducing the on-line optimization to mostly table lookups.

B. Thesis Contribution

In this work, the development of an energy management system for HEV is described; it is called single step dynamic programming technique (SSDP). This method is derived from a dynamic programming technique and is able to produce results very close to optimal ones. The Forward Dynamic Programming (FDP) requires that a forecast of the car torque requirement over the whole trip or part of it is available [2]. However, in real time the road and driving conditions are not known a priori. The chief advantage of SSDP over DP or other formal optimization methods is that it does not require the speed forecast of the whole drive cycle but requires only a one-step-ahead speed forecast. As such it can readily be implemented in real time to do a "near optimal" scheduling of the battery and fuel cell resources under charge sustaining (CS) and charge depleting (CD) strategies without revising any rule base or program code. Moreover, SSDP is faster than DP and has lower computational load. Unlike rule-based control, SSDP does not require to be tuned by engineers on new drive cycles or when new component technologies are introduced [12]. Moreover, it provides an easy mechanism to change from CS to CD operation simply by changing the lower bound of the state of charge (SOC) without the need to introduce an adaptive concept that selects an equivalent fuel consumption parameter required to manage the SOC to have a CS operation like in [12]. The SSDP is based on DP which can cater for non-linearity unlike quadratic programming used in [12].

The development of an artificial neural network (ANN) is also investigated in this thesis. The proposed ANN is trained based on optimal DP results carried out off-line. Unlike DP, the proposed ANN can be implemented in real time as it takes one step at a time. The solution of the ANN determines a near-optimal power split between the fuel cell

and battery indicating whether the battery should be charged or discharged and at what level. The proposed real-time control strategy may be a CS or CD strategy.

A one-step ahead speed forecast methodology is developed to determine the demand at the next period needed to solve SSDP and ANN. Different models are tested; higher order models (2nd, 3rd, and 4th orders) are able to forecast the speed with a small error but the 1st order model is able to produce better fuel saving results than higher order models since the net curve of the actual speed is only shifted by 1 step in this case. Therefore, the first order linear model also known as persistence forecast is used. Also by using a first order speed forecast model there will be no need to do an adaptive mechanism that adapts to changes in road conditions.

The organization of the rest of the thesis is as follows. In chapter 2 the system diagram is presented and explained. This chapter also includes a formulation of the optimization problem along with the system cost and constraints, where the DP and SSDP methods are discussed. Artificial neural network is investigated in chapter 3. The speed forecast model is described in chapter 4. The experimental results are presented and analyzed in chapter 5. Verification of the methodologies is provided by comparing them to results obtained using dynamic programming.

CHAPTER II

PROBLEM FORMULATION

A. System Diagram

The diagram of the electric power supply system of the hybrid electric vehicle (HEV) is shown in Fig. 1. The power supply of the vehicle has two sources: a fuel cell and a battery. The fuel cell is usually of the PEM (polymer electrolyte membrane) type getting H_2 from a high pressure tank that needs to be filled as a regular gasoline reservoir. The battery is connected to the electric bus bar (bus) by a two way charge controller allowing it to be charged or discharged depending on the operating conditions of the car. Torque and speed requirements of the mechanical drive system are satisfied by an induction machine taking 3-phase electricity through a pulse-width modulated (PWM) inverter with dc supply from the electric bus bar. The power output is usually controlled by increasing or decreasing the battery output power or the fuel cell output power. The varying speed requirements of the car are satisfied by switching frequency control of the inverter taking into consideration the gear ratio [2]. The "Near Optimal Control" block will use speed forecast information to know the speed of the car and the torque load at each period and then determine for each period the fuel cell and battery power levels taking into consideration the various constraints of power balance, power limits, SOC limits, and ramp rate limits. The output of the "Near Optimal Control" module is used by "Standard Vehicle Control" as a guide to schedule the resources over the next few seconds until the next update in the information.
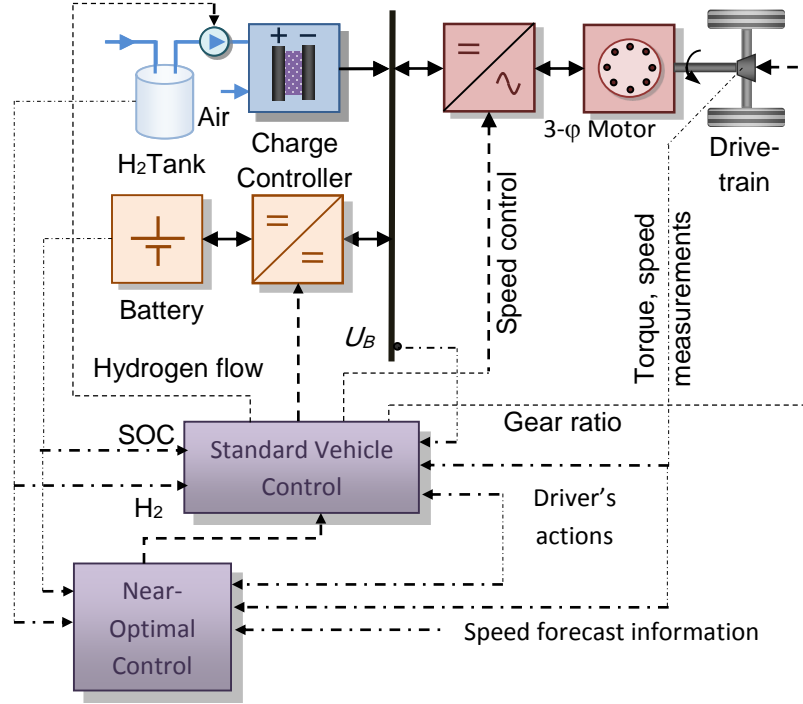
Figure 1: The system diagram of the FCHEV

B. Problem Formulation

The proposed module provides vehicle control with the recommended fuel cell and battery power levels that will minimize the cost of system operation during the up-coming trip. In this module the speed of the drive cycle is obtained from a one-step ahead speed forecast model. The power demand forecast at the wheels is obtained from the speed of the drive cycle, the basic car data and road topology. The power demand forecast at the dc bus is suitably obtained from that at the wheels considering the efficiency coefficients of the inverter, motor, and drive train as described by Rizzoni et al. [26]. The demand forecast is divided into N intervals, and during each interval k, $k = 1\ to\ N$, the power demand level,

D_k , and the power supply levels, from the fuel cell, F_k, and the battery, B_k, are assumed

constants. The duration or sampling time, ΔT, of each interval is given.

1. System Cost

The objective of the energy management system (EMS) is to determine for each

interval k the fuel cell power level, F_k, that minimizes the cost of operation consisting of

the sum of the hydrogen cost and that of the battery. The cost of fuel cell operation $\varphi_F(F_k)$

(in \$/h) is obtained from the hydrogen consumption rate curve (Fig. 2) by multiplying it by

the price of hydrogen taken at \$3/kg. The fuel cell cost curve has the same shape as the one

in Fig. 2 and may be approximated by a quadratic or cubic function. The curve shown

corresponds to a fuel cell of rated power of 58.8 kW and a net system peak efficiency of

55.6% occurring at 25% of rated power. The losses depicted in Fig. 2 have a figure of

about 10% at the rated value of power output [2].

The battery cost is used as a parameter to control the solution as either CS or CD.

Charge-sustaining operation, when battery losses are neglected, indicates that the net

energy over the long run from a battery is zero. In this case the average demand is being

supplied by the fuel cell, which is the alternative source in this case while the battery is

simply acting as a buffer. From the optimization viewpoint the battery cost is valued at an

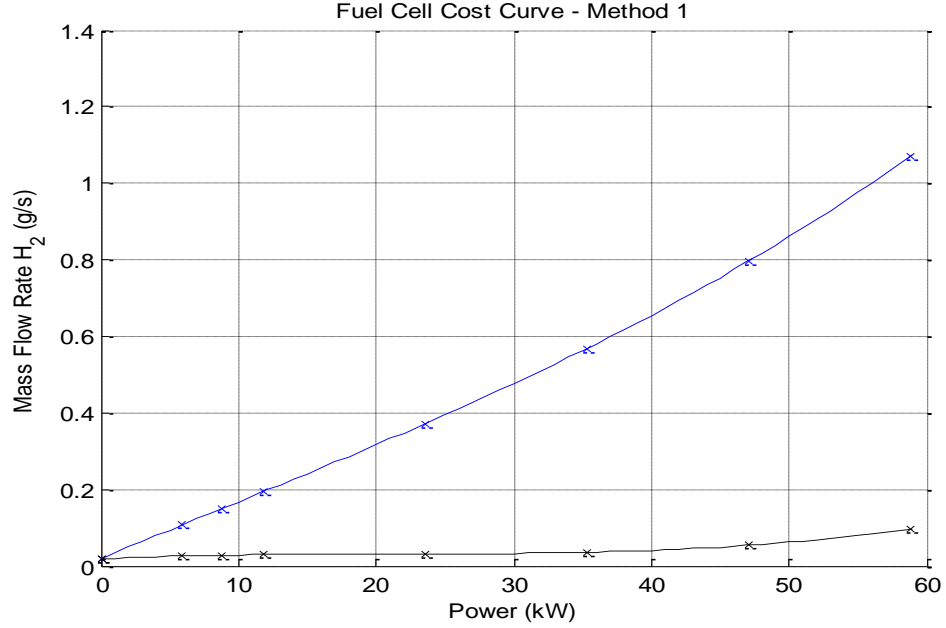incremental cost γ_{avg} in (\$/kWh) of the fuel cell evaluated at the average demand [2].

Figure 2: Hydrogen consumption curve (blue) and consumption loss (black) in g/s

Thus the system cost is given by:

$$\min \psi = \sum_{k=1}^{N} \left[\varphi_F(F_k) + \lambda_B \gamma_{avg} \, B_k (sign(B_k) + 1)/2 \right] \Delta T \qquad (1)$$

The battery cost parameter λ_B is varied to make the battery more or less attractive in supplying the power demand. It may be easily verified that there exists a value λ_{B0} that has a value around one, such that when $\lambda_B < \lambda_{B0}$ the apparent battery cost is cheaper than that of the fuel cell and thus the optimization process will tend to use more battery energy causing a CD strategy, and when $\lambda_B = \lambda_{B0}$ the battery energy will tend to zero leading to a CS strategy. A charge build up strategy may also be implemented when $\lambda_B > \lambda_{B0}$. Therefore, there exists a value of λ_B known as λ_{B0} at which the operation is exactly CS. This value is obtained by solving the DP iteratively which requires that the whole demand is known a priori which is not the case in real time. An easy but approximate mechanism

can be used instead to switch from CS to CD operation simply by changing the lower bound of the battery SOC. CS operation is obtained by enforcement of the lower bound on the SOC and CD operation is obtained by lowering the bound to the required depletion level. In both cases the battery cost parameter is set to a value lower than the incremental cost of the fuel cell at the average load of the car for the given drive cycle [2].

2. System Constraints

The minimization problem is subject to constraints:

$$F_k + B_k - D_k - R_k = 0 \tag{2}$$

$$X_k - X_{k-1} - \varphi_B(B_k)\Delta T = 0 \tag{3}$$

$$F_{min} \leq F_k \leq F_{max} \tag{4}$$

$$B_{min} \leq B_k \leq B_{max} \tag{5}$$

$$X_{min} \leq X_k \leq X_{max} \tag{6}$$

$$-R_F\Delta T \leq F_k - F_{k-1} \leq B_F\Delta T \tag{7}$$

$$-R_B\Delta T \leq B_k - B_{k-1} \leq B_B\Delta T \tag{8}$$

Equation (2) is the power balance constraint over each period k, where D_k and R_k are the estimated demand and brake power respectively. The second set of equality constraints (3) is that of the battery SOC change from one period to the next, where X_k is the battery SOC during interval k, and $\varphi_B(B_k)$ is the internal charge power (kW) obtained from the battery power map curve (Fig.3). Fig.3 shows the power curve for a battery rated at 49.6 kW with an energy storage capacity of 3.81 kWh based on data from the Li-ion VL 6Ah battery [2]. This curve can be obtained from the equivalent circuit of the battery

15

featuring the internal battery voltage and its series resistance [2]. The limits on power level

and state of charge are given by constraints (4), (5), and (6), where F_{max} is the rated power

of the fuel cell, B_{max} is the maximum power discharge of the battery, and B_{min} is the

minimum power charge and it is a negative value. The values X_{max} and X_{min} are the

operational limits on the state of charge required to keep the health of the battery. In

addition, realistic operating conditions have to respect the ramp-rate constraints given by

(7) and (8), where R_F and R_B are the ramp-rate limits in kW/s of the fuel cell and battery,
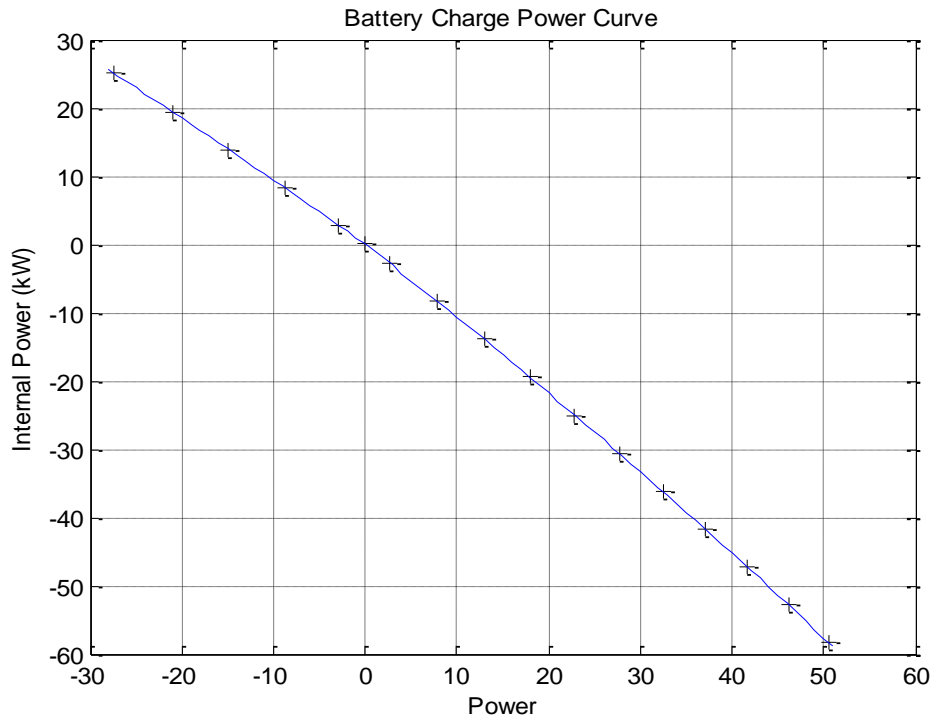
respectively.

Figure 3: Battery power map curve

B. Dynamic Programming

Forward Dynamic Programming (FDP) is well suited for this class of problems but is usually implemented using a heuristic to limit the number of levels of each stage to a fixed number in order to avoid the curse of dimensionality in problems with large number of stages and has been termed as approximate or tunnel dynamic programming (TDP). In this context, the power demand forecast curve will be divided in stages where at each stage the fuel cell power level can be in one of several discrete states. Thus for each state the battery power may be determined from the power balance constraint equation (2). Power limit constraints on the fuel cell are ensured by proposing discrete states in the range F^{min} to F^{max}; care must be taken to ensure that the discretization interval is smaller than the ramp rate of the fuel cell. Constraints on battery power (5) and ramp-rate constraints, (7) and (8), are enforced by a penalty cost method. The battery state-of-charge constraints (3) and (6) are also treated by applying a high penalty on infeasible states from among the set of proposed ones at a particular stage. The process is illustrated in Fig.4. For illustration purposes the fuel cell is assumed to be at one of 4 levels ($L = 4$), e.g. 100%, 66.7%, 33.3%, and 0% of full rating. At stage 1, the states corresponding to these levels are S_{11}, S_{12}, S_{13}, and S_{14}, respectively. There are transitions from each state to all the states of the following stage. In other words the matrix is full, but for clarity purposes only the transitions from the minimum state at each stage are shown in the figure. Darkly shaded states S_{11}, S_{12}, S_{21}, S_{31}, and S_{N1} have penalties associated with them and are unlikely to be in the optimal path which is found by back-tracing from the minimum state at the last stage, S_{N3}, for example.

The objective function (equation (1)) will be calculated for all the states of stage 1. Then for each state of subsequent stages (i.e. $k = 2$ to N), the possible transitions from the states ($j = 1$ to L) of the previous stage k-1 are identified, and the minimum cost of reaching each state is built recursively. Thus at each stage k, let the minimum cost of reaching each state $S_{k-1,j}$ be given by $\left(\hat{\psi}(S_{k-1,j}) \right)$ then the minimum cost of reaching state $S_{k,l}$ is given by:

$$\hat{\psi}(S_{k,l}) = \min_{j = 1, L} \left\{ C(S_{k-1,j}, S_{k,l}) + \hat{\psi}(S_{k-1,j}) \right\} \quad (9)$$

Where $(S_{k-1,j}, S_{k,l})$ with $j = 1$ to L are the possible transitions from the states $S_{k-1,j}$ to state $S_{k,l}$ and $C(S_{k-1,j}, S_{k,l})$ are their corresponding transition costs. For example, the possible transitions to state S_{23} are (S_{11}, S_{23}), (S_{12}, S_{23}), (S_{13}, S_{23}), and (S_{14}, S_{23}). The numbers on top of states S_{11}, S_{12}, S_{13} and S_{14} are the minimum costs for reaching these states from the previous stage. And the cost next to each transition is the cost of operating the system in period 2 at the demand level D_2. The cost of reaching state S_{23} is the minimum of the cost of the previous stage added to the cost of each transition, which is 2.4, i.e. minimum of $\{1.5 + 1.2, 1.3 + 1.2, 1.2 + 1.2, 1.3 + 1.2\}$. Then the ancestor state of S_{23} is S_{13}.
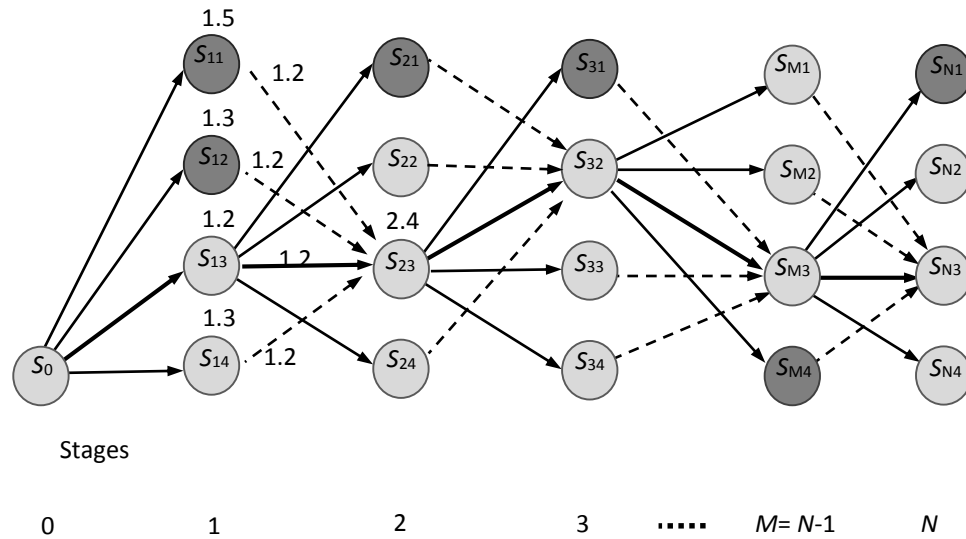
Figure 4: Dynamic programming

When the last stage is reached, the state with minimum cost is identified. Then the ancestor state leading to it is also identified and this is repeated to determine the optimal path by a trace-back procedure until state S_0 is reached. The heuristic used here to discretize the fuel cell output into L levels is essential in keeping the calculations of the DP algorithm within a manageable range. Decreasing the number of levels or states per stage would lead to approximate and thus "suboptimal" solutions, whereas increasing them would cause the computational requirement of the DP procedure to increase in some significant degree. Identifying a good compromise is essential for this class of problems, especially if real-time implementation is sought. The essential steps of the DP algorithm are given in List 1, where $\mathcal{M}$ a high cost is used as penalty, and **S** is the set of feasible transitions.

List 1: Dynamic Programming (DP) Algorithm

"At every stage 'k'

For $k= 1, N$

  "At every level 'l'

  For $l= 1, L$

$$F_{k,l} = F_{max} \, l/L \qquad \text{"Fuel cell power"}$$

$$B_{k,l} = \max(D_k - F_{k,l}, B_{min}) \qquad \text{"Battery power"}$$

$$C_F = \varphi_F(F_{k,l}) \qquad \text{"Fuel cell cost"}$$

$$C_B = \lambda_B \, \gamma_{avg} \, \text{sign}(B_{k,l} + 1)/2 \qquad \text{"Battery cost"}$$

$$C(S_{k-1,j}, S_{k,l}) = C_F + C_B \; \forall \, j \qquad \text{"Transition cost"}$$

"Set large penalty cost $\mathcal{M}$ for infeasible transitions"

$$\mathcal{P}_j = 0 \; \forall \, j$$

$$\text{If } \left((S_{k-1,j}, \, S_{k,l}) \notin \mathbf{S} \right) \Rightarrow \mathcal{P}_j = \mathcal{M} \; \forall \, j$$

"Minimum cost node in stage k"

$$\hat{\psi}(S_{k,l}) = \min_{j=1,L} \left(\hat{\psi}(S_{k-1,j}) + C(S_{k-1,j}, S_{k,l}) + \mathcal{P}_j \right)$$

$$\hat{A}_{k,l} = j_{k-1}^{min} \qquad \text{"Antecedent minimum cost node"}$$

  End

End

$$[\hat{F}, \hat{B}, \hat{X}] = \text{Trace\_Back}(\hat{A}, F, B) \qquad \text{"Trace back process"}$$

End

C. Single Step Dynamic Programming

The single step dynamic programming (SSDP) solution approach is derived from DP. The problem formulation is still the same; the power demand is also divided into stages and the fuel cell is divided into levels at each stage. The battery power is determined for each level from the power balance constraint (2). Power limit constraints on the fuel cell are ensured by proposing discrete states in the range F^{min} to F^{max}; care must be taken to ensure that the discretization interval is smaller than the ramp rate of the fuel cell. Constraints on battery power (5) and ramp-rate constraints, (7) and (8), are enforced by a penalty cost method. The battery state-of-charge constraints (3) and (6) are also treated by applying a high penalty on infeasible states from among the set of proposed ones at a particular stage.

The process is illustrated in Fig. 5. For illustration purposes the fuel cell is assumed to be at one of 4 levels ($L = 4$), e.g. 100%, 66.7%, 33.3%, and 0% of full rating. At stage 1, the states corresponding to these levels are S_{11}, S_{12}, S_{13}, and S_{14}, respectively. Darkly shaded states S_{11}, S_{12}, S_{21}, S_{31}, and S_{N1} have penalties associated with them and are unlikely to be in the optimal path.

SSDP differs from DP in that it is a forward-looking model that minimizes the system losses at every sample time. It allows the engine speed to move from the current speed to optimal target speed thus "chasing" the optimal speed target [12]. In this case the matrix is not full and there are transitions only from the minimum state of the previous stage to all other states of the next stage. Therefore, SSDP does not require the speed forecast of the whole drive cycle but requires only a one-step-ahead speed forecast. As such it can be readily implemented in real-time.
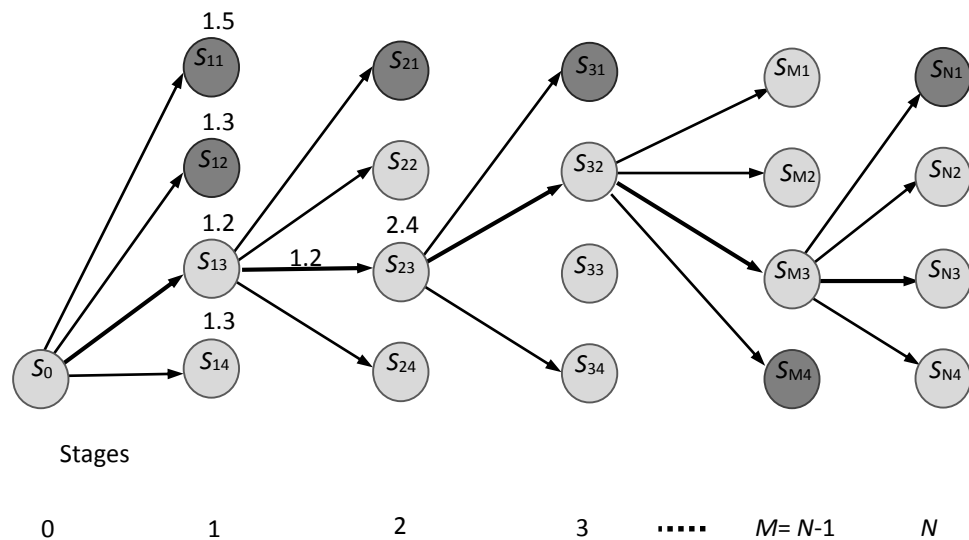

Figure 5: Single step dynamic programming

The essential steps of the SSDP algorithm are given in List 2, where $\mathcal{M}$ a high cost is used as penalty, and $\boldsymbol{S}$ is the set of feasible transitions.

The fuel cell cost, and battery cost are calculated for each state of stage k. The cost of transition from S_{k-1}, the minimum state at stage $k-1$, to $S_{k,l}$ is the fuel cell cost and battery cost of $S_{k,l}$. The constraints are checked for the transition from S_{k-1} to $S_{k,l}$ and in case of violation a penalty cost is added. The process is repeated for all the states of stage k.

Thus at each stage k, let the minimum cost of reaching stage $k-1$ be given by $\left(\hat{\psi}(S_{k-1}) \right)$ then the minimum cost of reaching stage k is given by:

$$\hat{\psi}(S_k) = \mathop{min}_{l\,=\,1,L} \left\{ C\left(S_{k-1}, S_{k,l}\right) + \hat{\psi}(S_{k-1}) \right\} \qquad (10)$$

Where $\left(S_{k-1,}, S_{k,l}\right)$ with $l = 1\ to\ L$ are the possible transitions from the state S_{k-1} to states $S_{k,l}$ and $C\left(S_{k-1}, S_{k,l}\right)$ are their corresponding transition costs. For example, if S_{13} is the minimum state in stage 1, then the possible transitions from stage 1 to stage 2 are (S_{13}, S_{21}), (S_{13}, S_{22}), (S_{13}, S_{23}), and (S_{13}, S_{24}). The numbers on top of states S_{11}, S_{12}, S_{13} and S_{14} are the minimum costs for reaching these states from the previous stage. And the cost next to each transition is the cost of operating the system in period 2 at the demand level D_2.

The state with minimum cost at stage k is included in the optimal path, and the whole process is repeated to identify the minimum cost at each stage.

List 2: Single Step Dynamic Programming (SSDP) Algorithm

"At every stage 'k'

For $k= 1, N$

For $l= 1, L$

$F_{k,l} = F_{max} \dfrac{l}{L}$ "Fuel cell power"

$B_{k,l} = max(D_k - F_{k,l}, B_{min})$ "Battery power"

$C_F = \varphi_F(F_{k,l})$ "Fuel cell cost"

$C_B = \lambda_B \, \gamma_{avg} \dfrac{sign(B_{k,l}+1)}{2}$ "Battery cost"

$C(S_{k-1}, S_{k,l}) = C_F + C_B$ "Transition cost"

"Set penalty to large cost M for infeasible transitions"

$P_l = 0$

$If \left((S_{k-1}, S_{k,l}) \notin S \right) \Rightarrow P_l = M$

End

"Minimum cost node in stage k"

$\hat{\psi}(S_k) = \min\limits_{l=1,L}\left(\hat{\psi}(S_{k-1}) + C(S_{k-1}, S_{k,l}) + P_l\right)$

End

The fuel cell incremental cost γ_{avg} given in equation (1) is calculated at average demand. In real time the average demand is not known. Equation (11) is used to update the average demand at each period, where $\bar{D}_k$ is the average demand at period k, $\bar{D}_{k-1}$ is the old average at period $k-1$, and $\hat{D}_k$ is the estimated demand at period k. The variable n is chosen by trial and error. Simulation results show that the average demand is not significantly affecting the results, so only few points are taken ($n = 4$). Small values of n give better results than larger ones since the response to changes on average will be faster.

$$\bar{D}_k = \frac{n-1}{n}\, \bar{D}_{k-1} + \frac{\hat{D}_k}{n} \tag{11}$$

Concerning λ_B which also appears in equation (1), it should be kept low for CD operation because when the battery is cheaper it will be depleted faster. However, for CS

operation λ_B does not make a big difference because the state of charge is bounded but better results are obtained when λ_B is close to 1 so that the battery cost is close to the fuel cell incremental cost. The relation between λ_B and battery remaining energy is shown in Fig. 6. For values of λ_B close to 1, CS operation is obtained as the battery remaining energy is close to the initial value which is 0.8, and for small values of λ_B CD operation is obtained. As λ_B increases the battery remaining energy increases until a saturation value is reached since the battery remaining energy depends on braking operation. HWFET approaches saturation before UDDS and has a lower remaining energy value because HWFET has less braking than UDDS. A value of λ_B around 0.82 is chosen for both CS and CD depletion operations since CD is obtained by lower bound relaxation not by lowering λ_B.
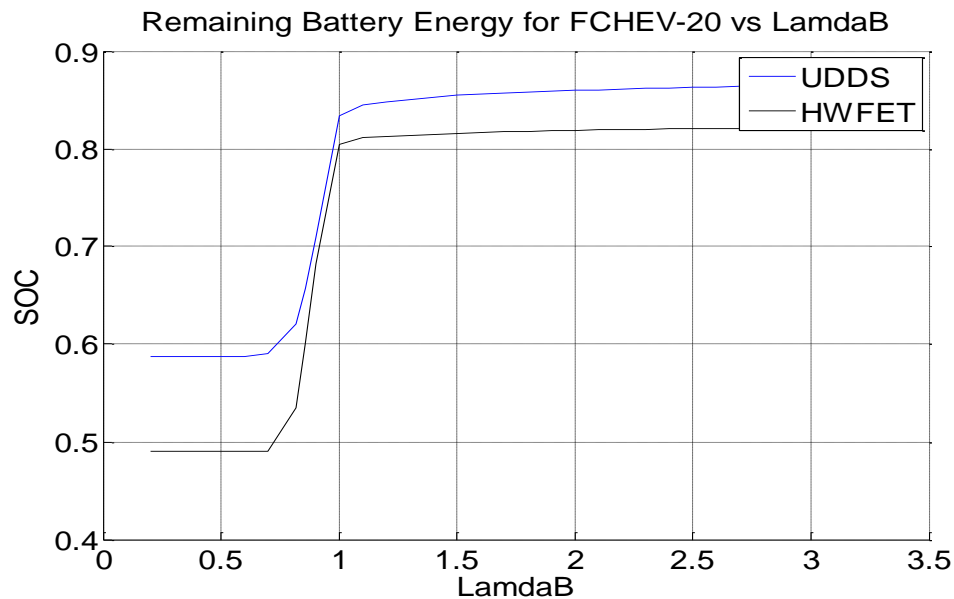

Figure 6: Battery remaining energy versus the battery control parameter $\boldsymbol{\lambda_B}$

CHAPTER III

ARTIFICIAL NEURAL NETWORKS

The artificial neural network (ANN) is an algorithm inspired from the biological human cortex. The multilayered neural network is a system made up of layers containing neurons; neurons in different layers are connected to each other forming a network. Each neuron is called a perceptron. Perceptrons receive signals from each other and pulse a signal as the output of an activation function (f). Each neuron has a bias (b), weight(w), and an activation function. The proposed ANN consists of three layers. The first layer is the input layer with three neurons corresponding to the number of inputs, the second layer is the hidden layer with 5 nodes, and the third layer is the output layer with one neuron corresponding to the system output as shown in Fig. 7.
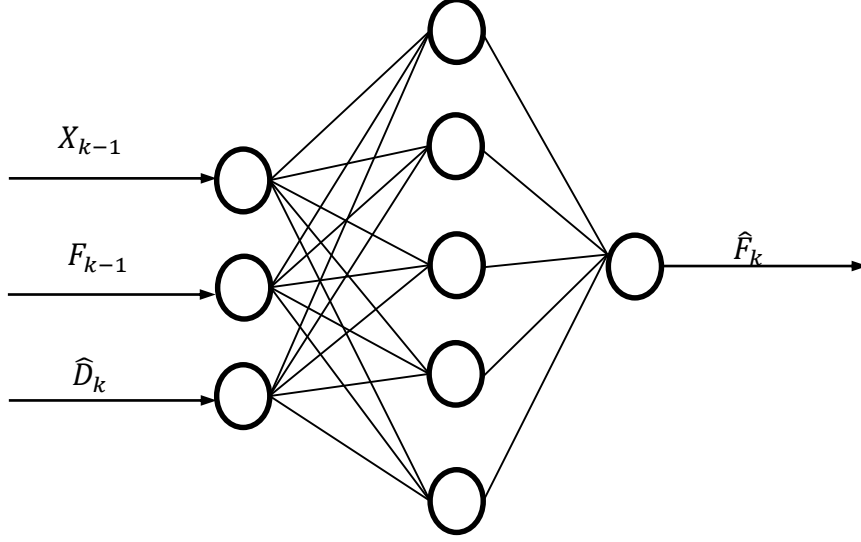
Figure 7: The architecture of the proposed ANN

The number of hidden layers and hidden nodes is chosen by trial and error. One hidden layer with five nodes is selected since it is able to produce the lowest hydrogen consumption thus satisfying the objective of the study. Smaller architectures produce better results in terms of hydrogen cost and hydrogen consumption which decrease as the number of hidden nodes and hidden layers decrease. On the other hand, larger architectures produce better results in terms of battery degradation and system cost. Since the main objective of the study is to reduce the consumption of hydrogen, a small architecture is chosen.

The inputs of the ANN are chosen to be the state of charge X_{k-1} at instant $(k-1)$, the fuel cell power F_{k-1} at instant $(k-1)$ and the estimated power demand $\widehat{D}_k$ at time (k). The demand requirement and battery state of charge are two important inputs. The battery state of charge determines whether the battery should be charged or discharged, and the estimated demand is needed to determine the required power at the wheels. The fuel cell

27

power at the previous period is included due to the fuel cell ramp rate, since the neural network should be able to learn the changes in the fuel cell level in order to avoid violations in the ramp rate. The battery ramp rate is not accounted for since it is much higher than that of the fuel cell.

The weights and biases are initiated randomly and are updated according to Levenberg-Marquardt optimization, which interpolates between the Gauss-Newton algorithm and the gradient descent [16]. The activation functions are chosen by trial and error; a log sigmoid activation function is used in the hidden layer and a linear activation function is used in the output layer. The classifier can be dominated by some attributes with relatively large numbers, to avoid this, features are normalized (e.g., mapped to numbers between 0-1). The ANN is trained using a dataset created by DP. The data set used for the UDDS drive cycle has 1370 instances in a three-dimensional feature space, where the features are: power demand, fuel cell power, and battery SOC.

The ANN is trained to learn the pattern of some instances obtained from DP results and then it is tested on new unseen instances where it should be able to produce results close to optimum ones. Therefore, the road is divided into two parts; training is done over one part consisting of 689 data points and testing is done over the other part. The number of data point over which training is done is chosen by trial and error. When few data points are chosen for training, the data in this case is not enough to train the model well. On the other hand, when too many data points are chosen for training, an overfit will occur preventing the ANN from being able to generalize well when it comes upon new unseen data.

The artificial neural network is used to find the fuel cell power at an instant (t). The battery power and the brake power can be determined from the power balance constraint as shown in list 3. The ANN results are compared to the optimum results of the dynamic programming applied over the same drive cycle and for the same vehicle. It is worthwhile noting that the first time the ANN is run the battery minimum state-of charge (SOC) is violated by around 75%. Therefore, the minimum allowable SOC is reduced from 0.8 used in DP to 0.75 allowing for some violations (soft margin) since ANN is a near-optimal solution of the energy management problem. Concerning the fuel cell power, the ANN produces some negative values which are forced to zero hence obtaining the power from the battery in these cases. To avoid violations of the power level constraints, all the fuel cell powers that are below minimum are set to F_{min}, but this caused the battery remaining energy to build up throughout the experiment instead of remaining constant thus violating the conditions of CS mode.

In an attempt to make the final and initial SOC match, the fuel cell power is calculated using ANN at each period. The obtained fuel cell power is corrected to satisfy limit and ramp rate constraints and then it is used to find the battery energy and SOC. The input of the ANN at the next period is updated by taking the obtained SOC and corrected fuel cell power from the previous period and so on. This method was not able to maintain a constant energy in the battery throughout the trip and the battery remaining energy followed an increasing pattern where the SOC increases above minimum by around 81.2%. Another attempt to solve the battery remaining energy problem is to increase the inputs of the ANN. A fourth input is added to the ANN to indicate whether the operation is CS or

CD (0 for Cs and $\alpha = \frac{SOC_0 - SOC_{final}}{SOC_{max}}$ for CD). Adding a fourth input is insufficient and the

SOC is not maintained in CS operation it increases above minimum in this case by about

98.3%.

Since all these methods are not able to maintain the SOC throughout the trip, the

initial network before modifications is considered i.e. before solving the fuel cell power at

each period and before adding a fourth input. However, in this case the fuel cell power is

allowed to go slightly below F_{min} (soft margin) due to the fact that ANN cannot handle

constraints like DP. This improves the battery remaining energy results in CS operation

mode, where the SOC increases above minimum at some periods by 0.78% thus

approaching towards the optimum solution as will be seen in the results section.

The same ANN network topology can also be used to operate in a CD mode

without having to change the architecture of the network, only the lower bound of the

battery SOC is changed. Also, the generalization capabilities of the ANN are checked. The

ANN is trained over the UDDS road and tested over the same drive cycle with a 10% faster

and 10% slower variations. It should be noted that in addition to the speed, the time interval

is changed to maintain a constant distance in all cases. The ANN is able to work reasonably

well when the speed of the UDDS cycle is changed. Cross-generalization is also performed,

where the ANN is trained over UDDS and tested over different drive cycles (HWFET and

NEDC). In both cases, the ANN is able to generalize fairly well. This shows that the same

network topology can be used for different cases and conditions.

List 3: Solve for Battery and Brake Power Algorithm

If $(D_k > 0)$
    $B_k = D_k - F_k$
    $R_k = 0;$
Else if $(D_k < 0)$
    $B_k = D_k - F_k$
    If $(B_k < B_{min})$
        "turn brakes on"
        $R_k = B_{min} - B_k$
        $B_k = D_k - F_k + R_k$
    End
Else
    $B_k = - F_k$
    $R_k = 0$
End

CHAPTER IV

SPEED FORECAST

One of the key functions of an effective hybrid fuel cell vehicle's design is the ability to model short-term predictions of traffic conditions on the roads. The impetus of forecasting traffic information, while relying on real-time information is to allocate the proportions of hydrogen and battery energies required throughout the trip in order to have the most efficient operation at minimum cost. Traffic information is usually reflected by traditional performance measures such as travel speed, time, and delays. Several traffic prediction models have been developed in literature using wide spectrum of modeling techniques. The main objective in this case is to be able to forecast the speed for a one step ahead.

For the SSDP and ANN approaches to be implemented in real time, a step-ahead forecast should be done in order to determine the demand at each period. The model used to forecast the speed is shown in equation (12). This model is a linear model of the forth order with a constant β_0, where V_k is the measured speed, V_{k-1} V_{k-2} V_{k-3} V_{k-4} are historical data, and β_0 β_1 β_2 β_3 β_4 are the beta coefficients.

$$V_k = \beta_0 + \beta_1 V_{k-1} + \beta_2 V_{k-2} + \beta_3 V_{k-3} + \beta_4 V_{k-4} \tag{12}$$

The beta coefficients are calculated from equation (13) using the pseudo inverse method (equation (14)), where V_m is the matrix of measured speed and H is the matrix of historical data.

$$V_m = H \times \beta \tag{13}$$

$$\beta = (H'H)^{-1}H' \tag{14}$$

To check the stability of the model several tests are done. The beta coefficients have been calculated for the UDDS drive cycle at medium speed and as the speed of the UDDS cycle increases or decreases for a forth order model with a constant (equation (12)). The results are shown in Table 1. The results show that only the constant β_0 changes as the speed of the drive cycle changes. This implies that β_0 is a kind of average speed that increases as the speed increase and decreases as the speed decrease. Therefore, to increase the model stability as driving conditions change, the constant β_0 will not be included.

As the driving cycle changes, the beta coefficients will change as shown in Table 2 where the coefficients of UDDS, NEDC, and HWFET drive cycles for a forth order model with a constant (equation (12)) are shown. Therefore, the beta coefficients suitable for one drive cycle will not be optimal for the other. Hence, there is no choice of the parameters that can be performed only once as initialization of the control strategy and applied in every situation. During real time operation, the optimization method uses those values of beta that are representative of the current driving conditions. This can be done by storing in the controller certain values that are typical of urban, highway, etc. drive cycles since it is difficult to calculate beta coefficients in real time because they depend upon the measured speed (equation (13)) which is not known a priori. To further check the stability of the model, the beta coefficients of UDDS are used to forecast the speed of HWFET and the speed of NEDC drive cycles. It seems that the beta coefficients are not significantly affecting the results and hence the model can be considered stable.

Table 1: The Beta Coefficients for UDDS Drive Cycle of Different Speeds

Beta coefficient	Slow	Medium	Fast
β_0	0.0558	0.062	0.0682
β_1	2.0479	2.0479	2.0479
β_2	-1.2107	-1.2107	-1.2107
β_3	0.1397	0.1397	0.1397
β_4	0.0161	0.0161	0.0161

Table 2: The Beta Coefficients for UDDS, NEDC, and HWFET Drive Cycles

Beta coefficient	NEDC	UDDS	HWFET
β_0	0.0091	0.062	0.0189
β_1	1.9299	2.0479	2.0865
β_2	-0.9434	-1.2107	-1.159
β_3	-0.01	0.1397	-0.0421
β_4	0.0214	0.0161	0.1126

When models of different orders are tested, the models with high orders appear to be better in terms of forecast (lower error), but when it comes to the implementation of the model with SSDP, the 1st order produces better fuel saving results since the net curve of the forecasted speed is only shifted by 1 step from the actual speed. This shows that there is no need to sophisticate the method; therefore, a first order model without a constant also known as persistence forecast given in equation (15) is used.

$$V_k = V_{k-1} \qquad\qquad (15)$$

When using a 1st order model, $\beta = 1$ which means that no adaptation mechanism is needed to adapt to changes in the road conditions. Moreover, the forecast time will not be considered since the forecasted speed at a certain instant k is simply the actual speed at instant $k - 1$.

The forecasted speed obtained is used to determine the demand required at the wheels which is used for solving the real time optimization methods (SSDP and ANN). The

forecasted speeds with negative values are set to zero before using them to solve the SSDP

or ANN method. Non-linear models are used in literature [27], but since the linear model is

producing good results non-linear models are not considered in this work.

CHAPTER V

SIMULATION RESULTS

The ANN and SSDP will be tested and compared to optimum results obtained by DP in order to provide an overall check of these methodologies. The tests will be carried over UDDS, HWFET, and NEDC drive cycles shown in Figs. 8, 9, and 10 respectively along with the power demand at these roads. The types of cars simulated have varying battery sizes to provide an all-battery range (ABR) of 10 to 40 miles and other component sizes are appropriately selected. The data of the cars used are shown in Table 3 [2]. The last two digits of the car-type indicate the all-battery range (ABR) in miles for the corresponding type. The power demands shown in Figs. 8, 9, and 10 correspond to the FCHEV-20, shown in row 2 of Table 3.
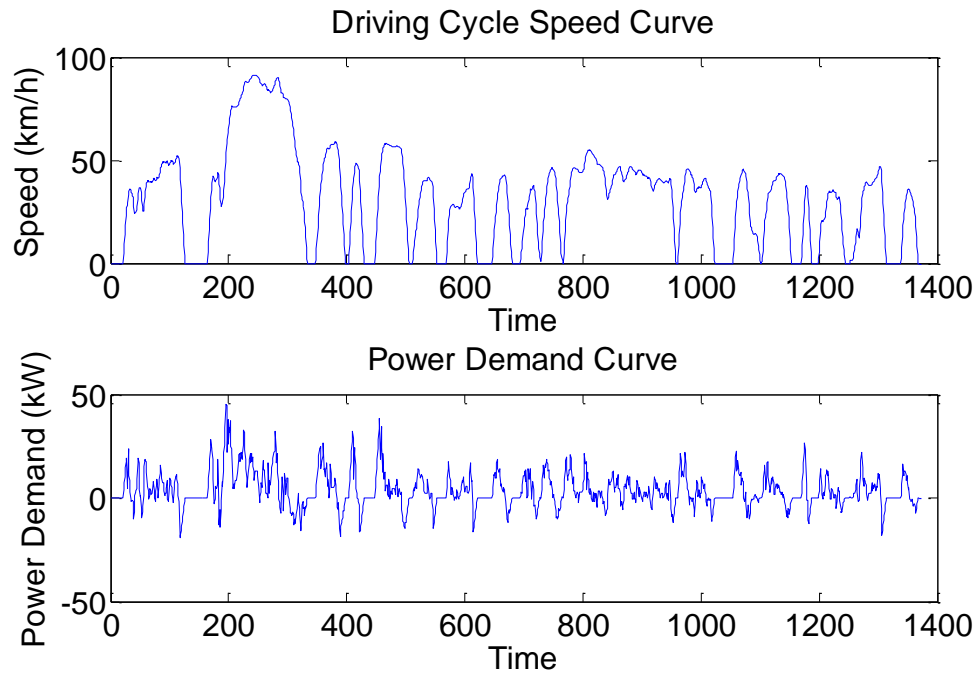
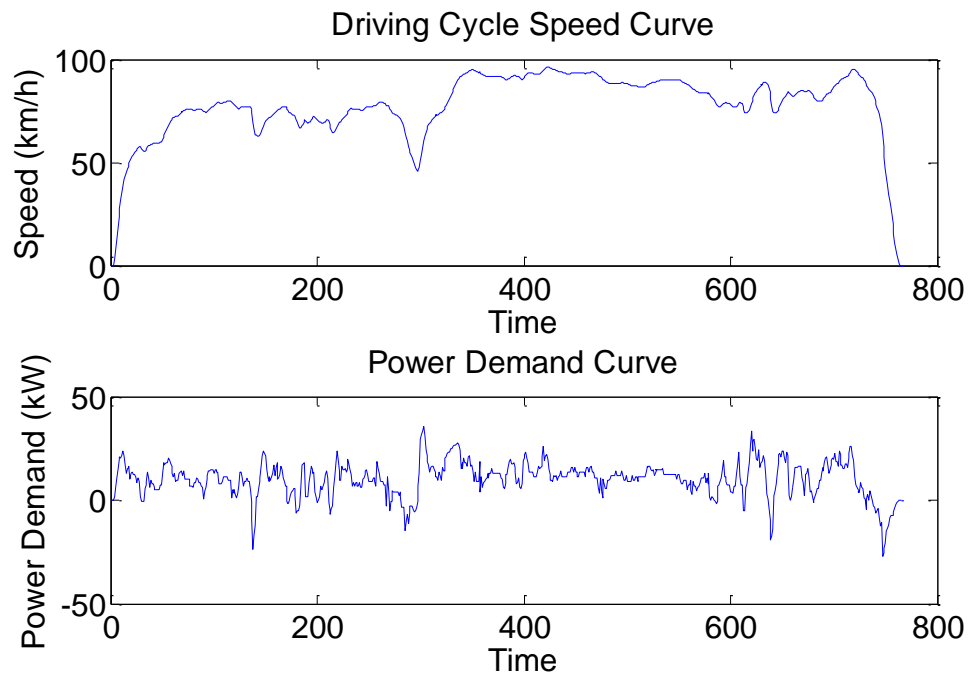Figure 8: The speed curve and power demand curve of the UDDS driving cycle

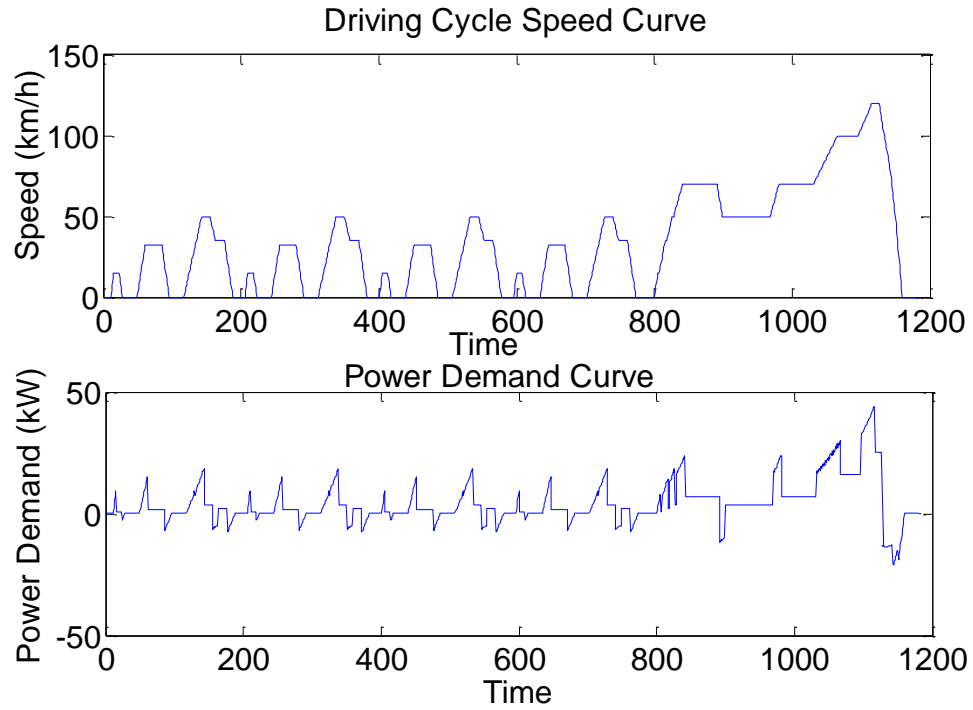Figure 9: The speed curve and power demand curve of the HWFET driving cycle

37

Figure 10: The speed curve and power demand curve of the NEDC driving cycle

Table 3: Power and Storage Components Sizes of Simulated Cars

Vehicle	ABR	Mass (kg)	Fuel Cell (kW)	Battery Energy (kWh)	Battery Power (kW)
FCHEV	00	1582	78.9	1.07	26.9
FCHEV	20	1591	58.8	7.57	50.6
FCHEV	40	1715	56.5	15.1	140.2

A. Single Step Dynamic Programming Results

The comparison between the SSDP and DP methods is carried out over the UDDS and HWFET drive cycles for the FCHEV-20. Table 4 compares SSDP to DP for charge sustained (CS) operation mode. Comparing SSDP with DP when the actual speed is used

i.e. the first two columns of Table 4, the H_2 consumption increases by 1.6% and 0.45% with

SSDP for UDDS and HWFET respectively. The battery degradation is higher by 17.8% and

31.3% for UDDS and HWFET respectively. The relatively high variations in the battery

degradation cost are due to the SOC slightly going below minimum in some periods as will

be seen in Fig. 14. The higher H_2 consumption and battery degradation caused the system

cost when applying SSDP to increase by 7.4% and 3% over UDDS and HWFET

respectively. SSDP and DP have the same battery remaining energy over UDDS and

HWFET which implies that over both drive cycles SSDP is able to restore the battery SOC

at the end of the cycle thus satisfying CS constraints. When the speed forecast is actually

used to solve SSDP, the results obtained are close to those obtained when actual speed is

used to solve SSDP where the system cost increases by 0.5% for UDDS and decreases by

0.4% for HWFET. The speed is forecasted using a first order linear model, also known as

persistence forecast. Comparing the fuel economy results obtained when using DP to those

obtained when using SSDP with forecasted speed, the system cost obtained for UDDS is

higher by around 6.9% and for HWFET it is higher by around 3.4%. This shows that the

speed forecast model is capable of producing results close to the optimum ones with a low

error, because the forecasted speed is obtained by shifting the net curve of the actual speed

by one step when a first order linear model is applied.

Table 4: DP and SSDP Results for FCHEV-20 over UDDS and HWFET-CS with $SOC_0= 0.8$

		DP Actual Speed	SSDP Actual Speed	SSDP Forecasted Speed
UDDS	H_2 cost ($)	0.2668	0.2711	0.2701
	Battery degradation ($)	0.1503	0.1770	0.1757
	System cost ($)	0.4171	0.4481	0.4458
	H_2 consumption (g)	88.94	90.37	90.04
	Battery Remaining energy (pu)	0.8014	0.8014	0.8014
HWFET	H_2 cost ($)	0.3760	0.3776	0.3778
	Battery degradation ($)	0.0339	0.0445	0.0461
	System cost ($)	0.4098	0.4221	0.4239
	H_2 consumption (g)	125.32	125.88	125.93
	Battery Remaining energy (pu)	0.8082	0.8082	0.8082

Figures 11 and 12 show the different power levels and velocity when the battery is operated in a CS mode over a portion of the UDDS with DP and SSDP respectively. The battery energy looks sustained in both cases as over the shown portion of the cycle the net battery energy seems to balance out as the positive areas (discharge) is about equal to the negative areas (charge). The battery is then charged from a braking operation over the time range from about 383 to 398 seconds. Also in both cases the battery plus the fuel cell powers are larger than the demand in absolute value term. At about 360s there is a sharp drop in the power demand of about 10.6kW, which is larger than the fuel cell ramp rate of about 7.8kW/s. The DP system prepares for this by increasing the battery power prior to 360s, so that it can contribute to the required rapid power demand drop as shown in Fig. 11 which is not the case with SSDP as shown in Fig. 12.
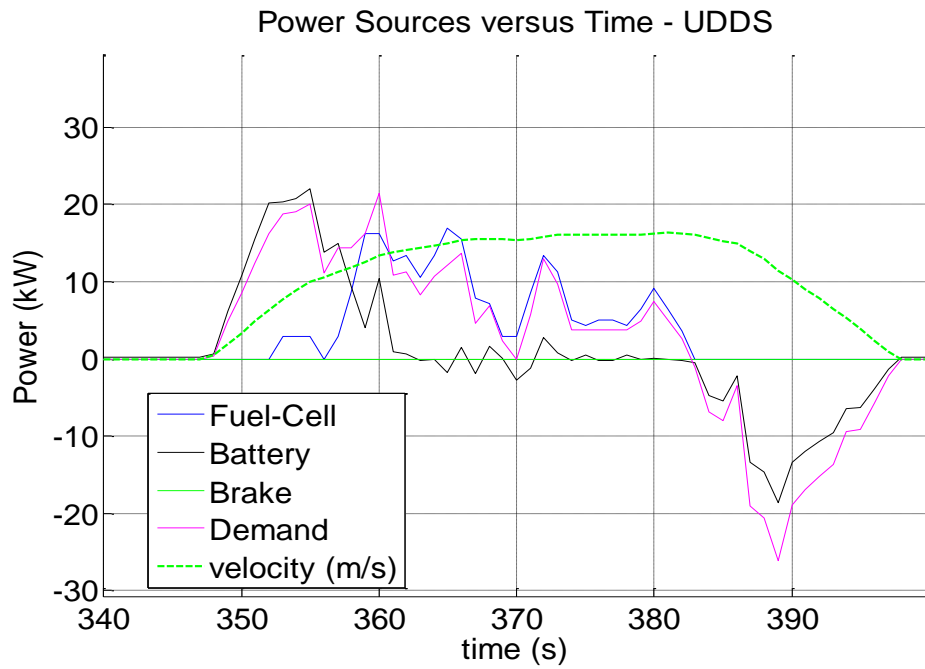
Figure 11: Power levels and velocity on part of the UDDS cycle for DP-CS strategy
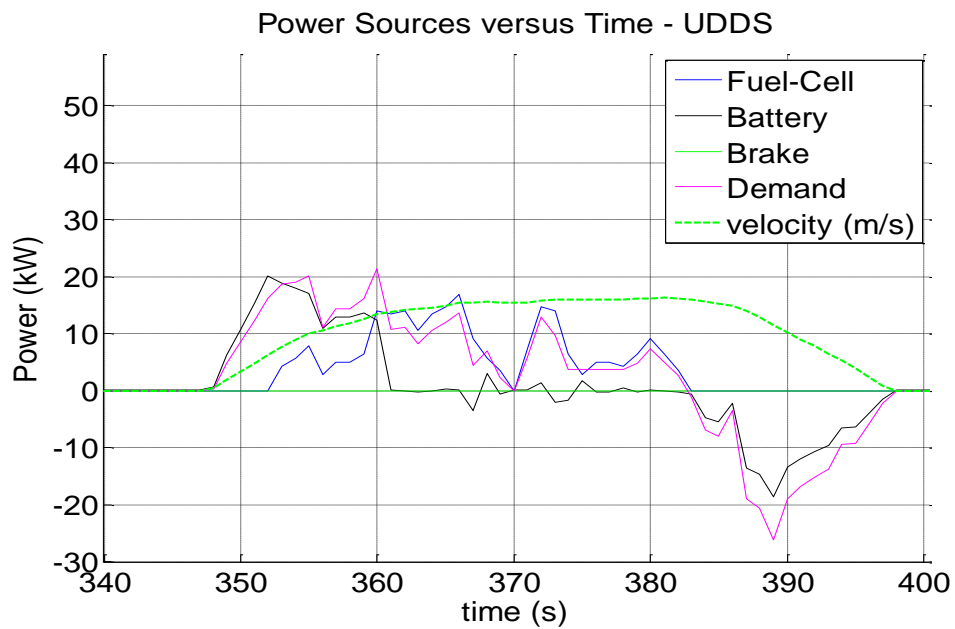

Figure 12: Power levels and velocity on part of the UDDS cycle for SSDP-CS strategy

The battery and fuel cell remaining energy are shown for DP and SSDP in Figs. 13 and 14 respectively. Since this is a CS operation, the battery remaining energy curve is examined to check if CS constraints are obeyed. The DP results show that the battery SOC is maintained throughout the drive cycle and it does not go below the minimum value which is set to 80% of the battery SOC i.e. equal to 6.056kWh. However, at the end of the cycle the SOC tends to rise slightly above minimum due to the last braking operation. On the other hand, when applying SSDP the battery SOC decreases below the minimum value at some periods around 197, 456, and 1176 seconds. The violation is very small around 0.2%. At the end of the drive cycle, the SOC is maintained but slightly higher due to the last braking operation like in the case of DP. According to [17], it is normal that the SOC deviates from the minimum value during the vehicle operation as long as the final SOC is maintained.
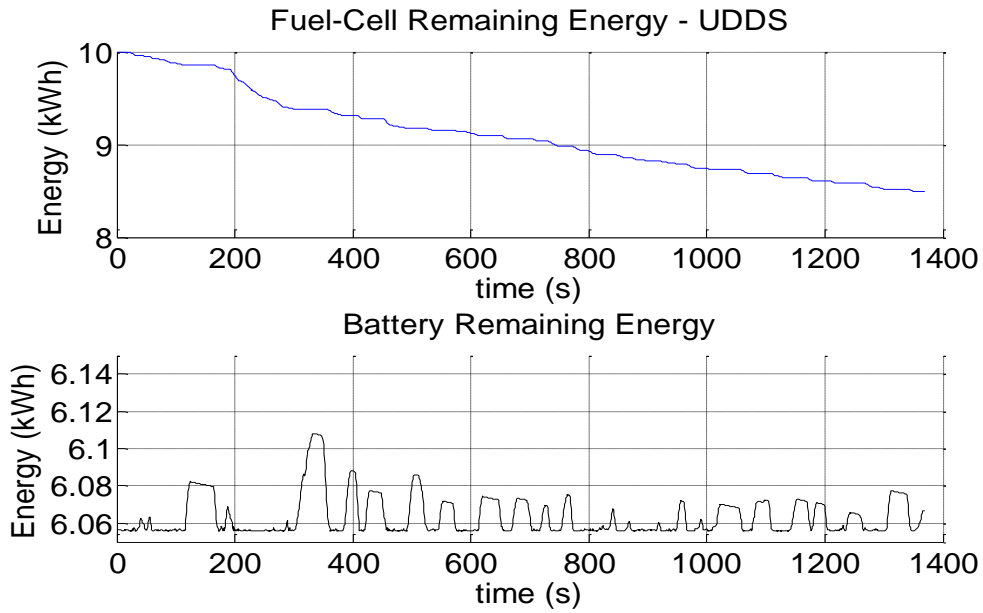
Figure 13: FC and battery remaining energy for DP over UDDS-CS
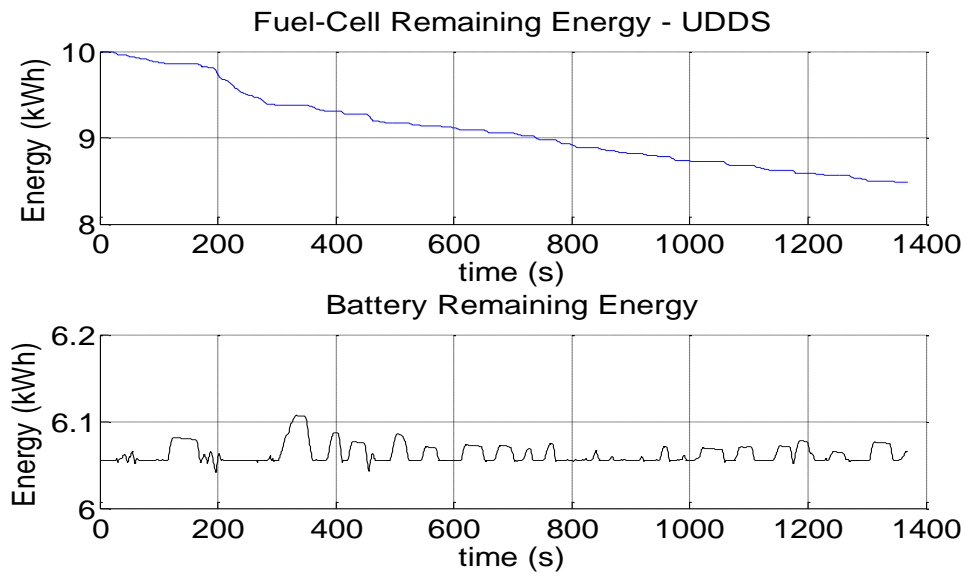

Figure 14: FC and battery remaining energy for SSDP over UDDS-CS

For CD mode, the results are shown in Table 5. Comparing SSDP to DP when actual speed is used, the system cost decreases by around 4% with SSDP for UDDS drive

cycle. This might be attributed to the battery being used less with SSDP where the battery remaining energy is slightly higher than that of DP. The decrease in the battery degradation resulted in a decrease in the overall system cost in case of SSDP. Concerning H_2 consumption, it increases by around 58% for UDDS when applying SSDP and by around 4.6% for HWFET.

Table 5: DP and SSDP Results for FCHEV-20 over UDDS and HWFET-CD with $SOC_0=$ 0.9

		DP Actual Speed	SSDP Actual Speed	SSDP Forecasted Speed
UDDS	**H_2 cost ($)**	0.0371	0.0585	0.0581
	Battery degradation ($)	0.6045	0.5579	0.5568
	System cost ($)	0.6416	0.6164	0.6149
	H_2 consumption (g)	12.37	19.49	19.35
	Battery Remaining energy (pu)	0.7014	0.7211	0.7214
HWFET	**H_2 cost ($)**	0.1390	0.1454	0.1452
	Battery degradation ($)	0.4952	0.5012	0.4999
	System cost ($)	0.6343	0.6466	0.6451
	H_2 consumption (g)	46.34	48.47	48.39
	Battery Remaining energy (pu)	0.7083	0.7082	0.7082

The battery and power levels for CD mode over portion of the UDDS are shown in Figs. 15 and 16 corresponding for DP and SSDP respectively. The power demand is being supplied mainly from the battery when applying DP as shown in Fig. 15. The fuel cell operates briefly between 352 and 361 seconds driven by the economic differentials in the costs. However, with SSDP the fuel cell operates between 352 and 367 seconds showing

that more fuel is being consumed as compared to DP and hence in this case the battery is
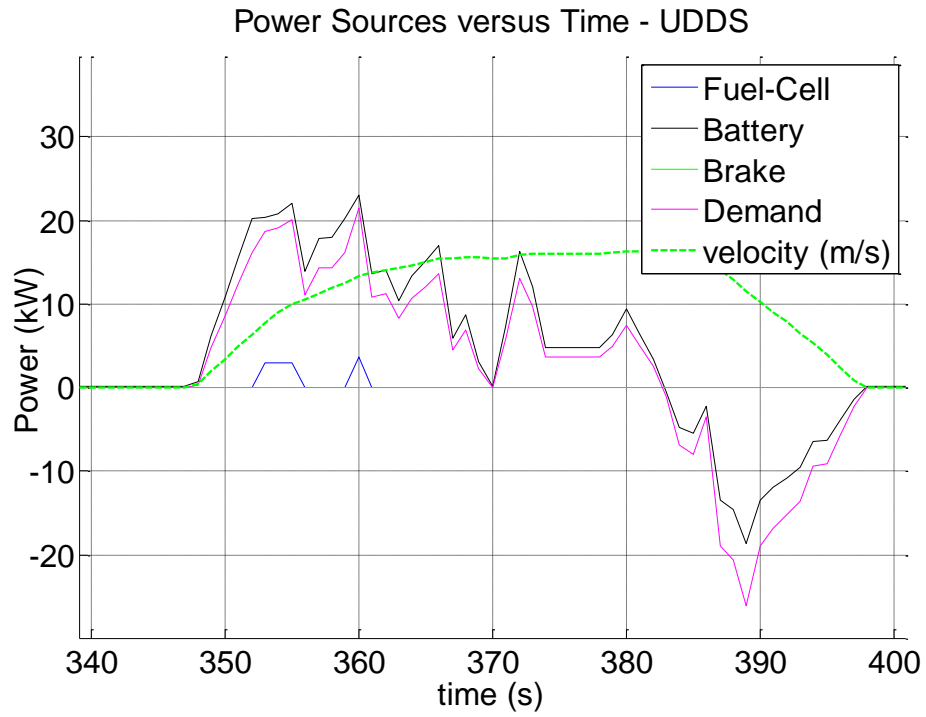
used less.

Figure 15: Power levels and velocity on part of the UDDS cycle for DP-CD strategy
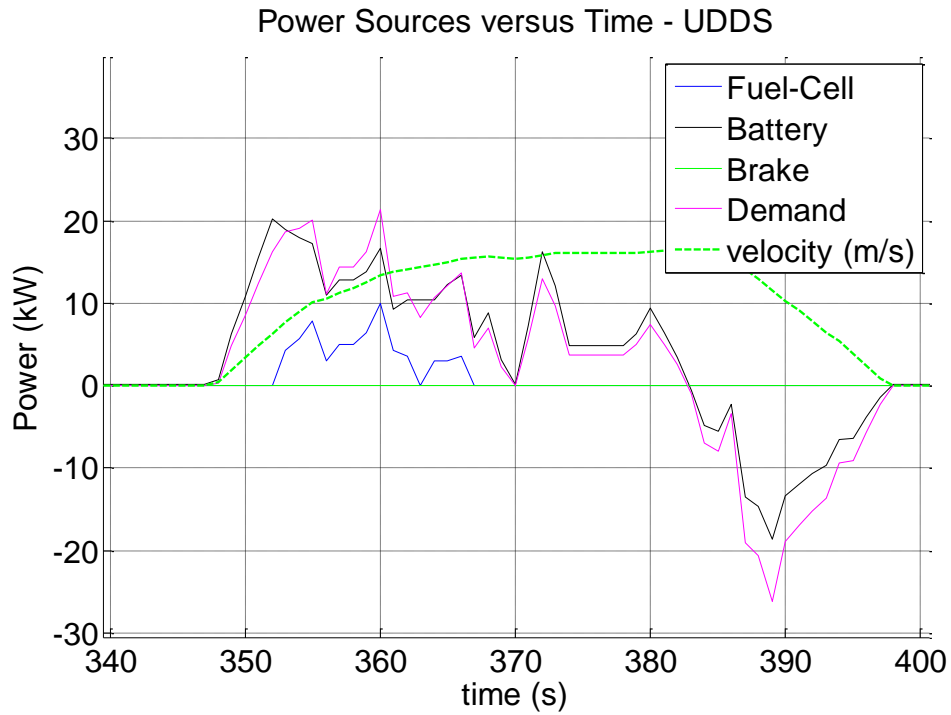
Figure 16: Power levels and velocity on part of the UDDS cycle for SSDP-CD strategy

For the CD mode, the fuel cell remaining energy should be examined to check if CD constraints are not violated. In Figs. 17 and 18, the fuel cell and battery remaining energy for DP and SSDP methods respectively are shown. The fuel cell energy is reduced from 10kWh to 9.9kWh with DP; whereas it is reduced further to around 9.78kWh with SSDP making slight difference between the two methods.
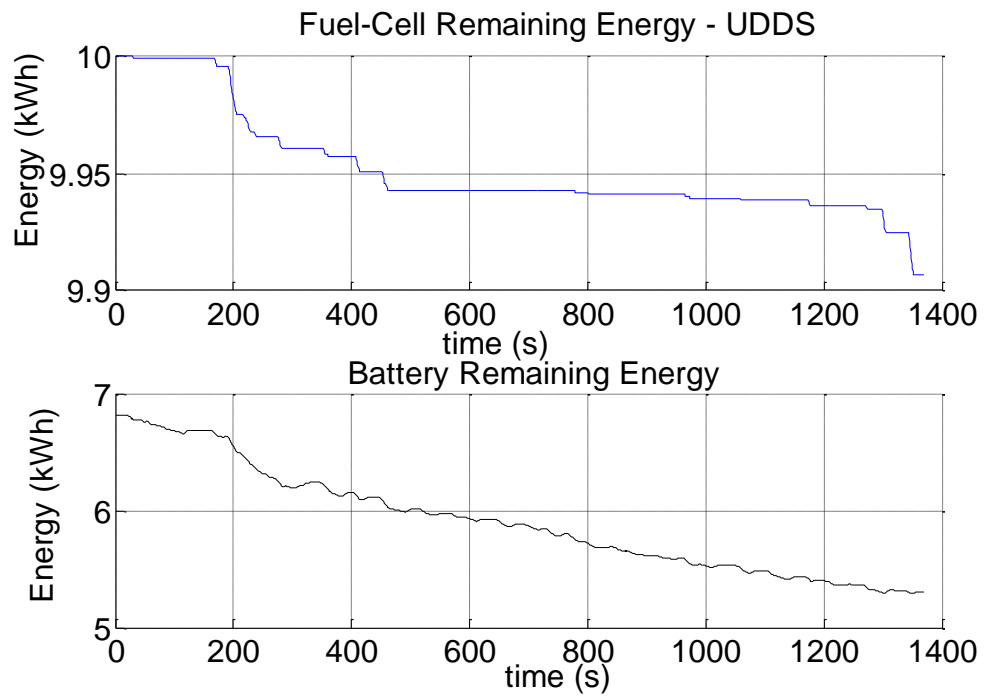
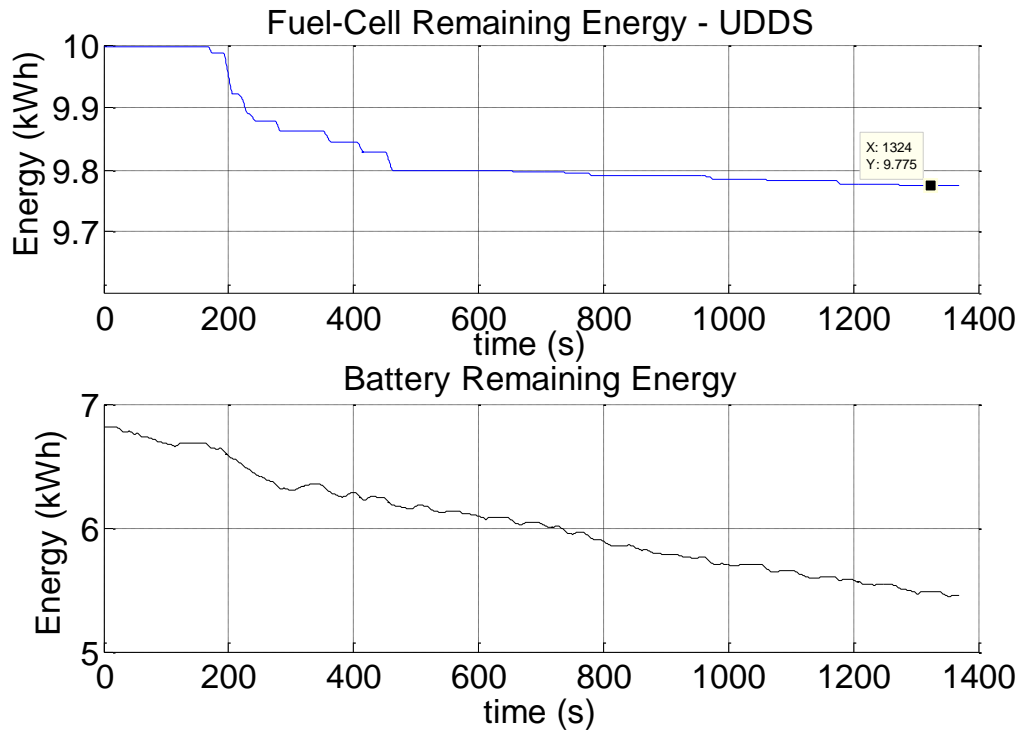Figure 17: FC and battery remaining energy for DP over UDDS-CD

Figure 18: FC and battery remaining energy for SSDP over UDDS-CD

Fig. 19 compares the optimal path obtained by DP to that obtained by SSDP for a portion of the road over the UDDS cycle for a CS operation. The two paths differ from each other at periods 353, 354, 355, and 356 where more fuel cell is consumed when SSDP is used.
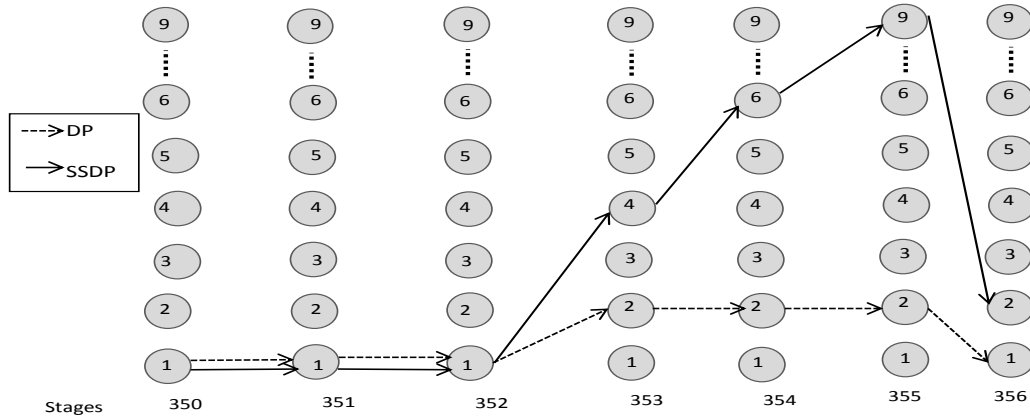
Figure 19: The optimal path obtained by DP compared to that obtained by SSDP over portion of UDDS-CS

The difference between the DP and SSDP results is because DP is a backward-looking model that allows only for feasible solutions by solving all possible optimal controls to fill the optimal field. Whereas SSDP is a forward-looking model that considers the constraints and instantaneously makes decisions for the entire system i.e. it minimizes the system losses at every sample time [12]. In this case some solutions might not be feasible because their associated penalty cost might be higher than the penalty cost of other solutions that are not considered, since SSDP considers only the solution with minimum cost at each period and not all the possible optimal controls like in DP.

The SSDP method mathematically has some infeasibility since it is a forward looking program as mentioned earlier. However, physically the SOC infeasibility is not serious because it is very small and this can be deduced by examining Fig.14 where the SOC is slightly going below minimum by around 0.2%. It should be noted that the violations are only SOC and there are no fuel cell ramp rate violations. This does not lead to infeasible solution because the battery usually has enough ramp rates and the limit on the

battery SOC is used to determine whether the operation is CS or CD. It should be noted that when the mode of operation is CD, the SSDP is able to find the optimum solution; this might be due to the SOC limits being more relaxed in this case.

Changing the number of levels affects the number of infeasibilities, the size of the added penalties for the corresponding infeasibilities, and the system cost. In this work, 81 levels are used as in [2]; however different values for the number of levels are tested to determine the effect of the number of levels on the system cost and infeasibility. As the number of levels increases the number of infeasibilities decreases until it reaches saturation at around 161 levels where 108 violations are obtained compared to 178 violations obtained at 21 levels. Also the size of added penalty is reduced with increasing number of levels. Although the number of violations decreases as the number of levels increase, only 106 violations are obtained at 81 levels. Concerning the system cost, it is reduced as the number of levels increases until a saturation is reached at 641 levels where the system cost is 0.4446$ as shown in Fig. 20. However, the change in the system cost is not significant as it is less than 10%. The accuracy obtained at 81 levels is enough knowing that the execution time increases as the number of levels increase to reach 11.63 sec at 2561 levels compared to 0.19 sec at 21 levels. Therefore, identifying a good compromise between accuracy and execution time is essential.
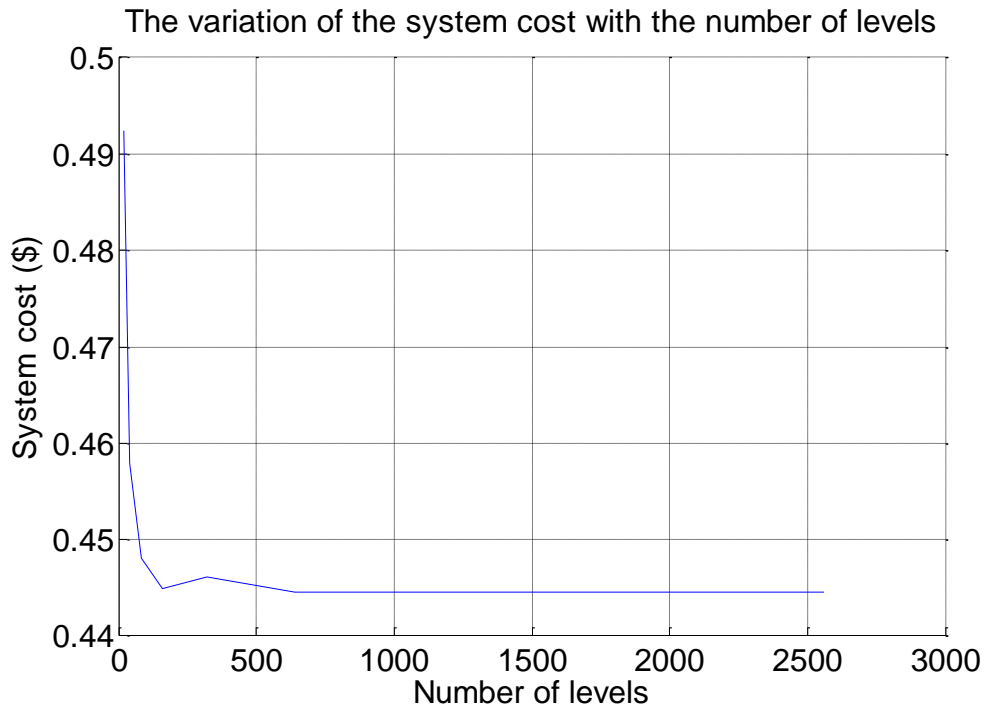
Figure 20: The variation of the system cost with the number of levels

The performance comparison with the various FCHEV is shown in Table 6 for the UDDS cycle. The results of the DP method tend to give solutions with lower hydrogen consumption depicted by the increased mileage per gallon of gasoline equivalent (mpgge) for CS operation and lower battery degradation depicted by increased watt-hour/mile (Wh/mi) for CD operation. This is expected since DP gives optimal results.

It should be noted that the SSDP method is faster than DP by 86.83% and has lower computational load. Also SSDP differs from DP in that it can be implemented in real time. Moreover, the performance in terms of fuel economy are practically very close for SSDP and the optimal DP, thus it can be asserted that a very slightly sub-optimal solution can be achieved with a technique much simpler than the one leading to the optimal policy.

Table 6: Performance of DP and SSDP for Various FCHEV over UDDS

Car Type	Method	CD (mpgge)[1]	CD (Wh/mi)	CS (mpgge)
FCHEV-0	DP SS			81.21 79.47
FCHEV-20	DP SS	600.86 381.34	201.73 181.70	83.56 82.25
FCHEV-40	DP SS	1031.7 487.04	221.39 199.48	79.8 78.28

B. ANN Results

The ANN at this stage is trained over UDDS drive cycle, and the vehicle used is

FCHEV-20. The comparison between the DP and the ANN results for CS mode over

UDDS drive cycle for the same vehicle is summarized in Table 7. Table 7 shows that the

hydrogen consumption and hence hydrogen cost in case of ANN are slightly higher than

that of the DP by around 3.6% resulting in slightly lower battery degradation with ANN by

around 12.7%. Therefore, the system cost in both methods is very close, as it increases

when ANN is used by around 2.23%. Concerning the final energy remaining in the battery,

it is closer to the initial energy (0.8) in case of DP than in the case of ANN which is

expected as DP can handle constraints easily. Fig. 21 shows that with ANN the SOC is

going slightly above minimum at some periods by around 0.78%, and the SOC is not

maintained throughout the drive cycle like in the case of DP or SSDP due to the suboptimal

nature of ANN that is not able to handle constraints. However, ANN is able to slightly

maintain the battery remaining energy in the CS operation since there is no significant

charge build-up or charge depletion.

Table 7: DP and ANN Results over UDDS-CS with SOC0=0.75

Parameters	DP	ANN
H_2 cost ($)	0.2669	0.2766
H_2 consumption (g)	89.0	92.2
Battery Cost ($)	0.1503	0.1312
System Cost ($)	0.4171	0.4078
Battery remaining energy (pu)	0.8014	0.8103
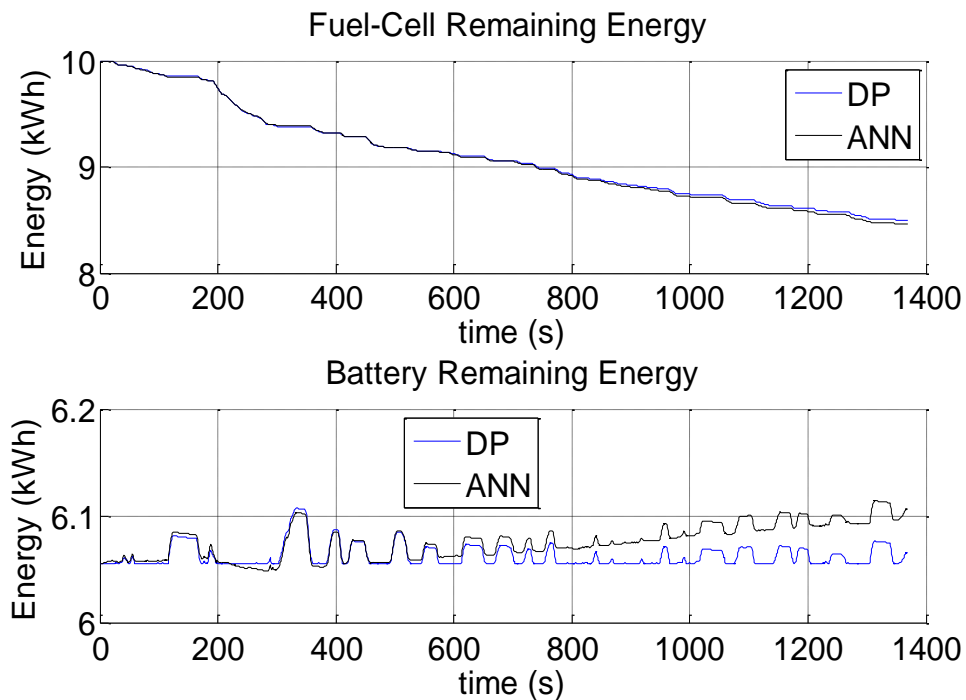
Figure 21: The FC and battery remaining energy for DP and ANN over UDDS-CS

Fig. 22 compares the fuel cell power level output obtained by an ANN to that

obtained by a DP over a portion of the UDDC cycle. The two results approximately follow

the same trend; however, they are shifted. The ANN results are able to follow the DP results at most periods, but at some instants the fuel cell power obtained by DP is zero whereas it is positive by ANN. Also at some periods the fuel cell obtained by ANN is negative, but these values are corrected and forced to zero. In general, the ANN solution is not the same as DP and this is expected but it is very close and does not show significant or abnormal trends.
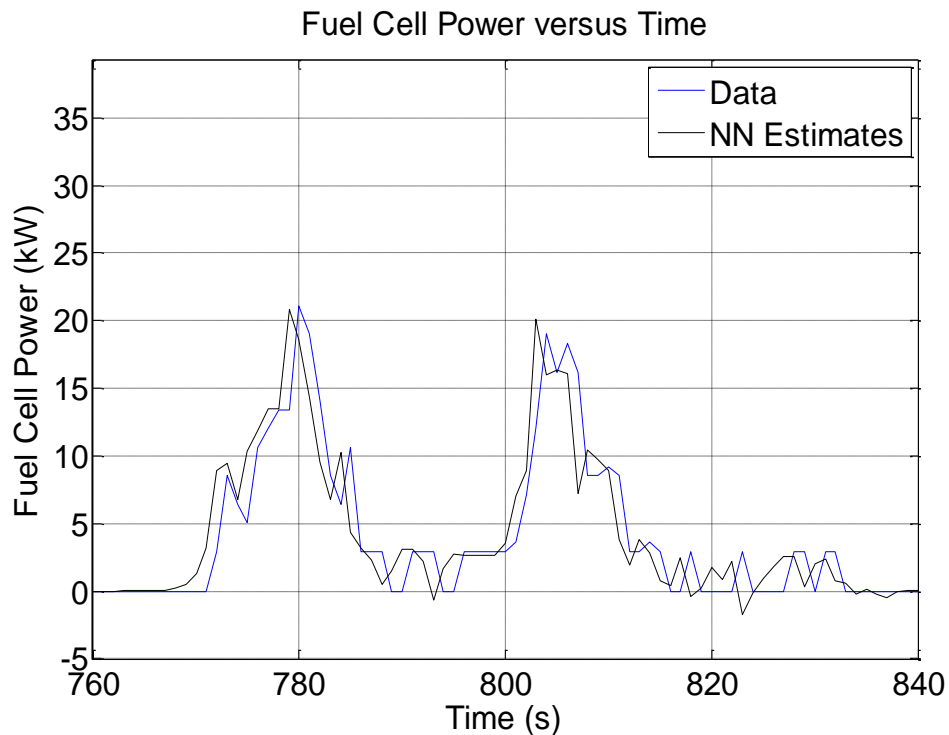

Figure 22: The FC power estimates for DP and ANN over UDDS-CS

The same network topology can be used to run a CD mode. Table 8 compares the ANN results to those obtained by DP over UDDS for CD mode of operation. The H_2 consumption in case of ANN is lower than that of DP by around 12% resulting in a lower H_2 cost. Whereas, the battery is used more when using ANN where the battery remaining

energy of ANN is slightly lower than that of DP by 0.57%, this caused the battery

degradation cost when using ANN to increase by around 1%. Therefore, the system cost

with ANN slightly increases as compared to DP by around 0.75%. Although, ANN does

not violate the CD constraints by utilizing more battery but this might violate the SOC

limits.

Table 8: DP and ANN Results over UDDS-CD with SOC0=0.9

Parameters	DP	ANN
H_2 cost ($)	0.0371	0.0327
H_2 consumption (g)	12.37	10.89
Battery Cost ($)	0.6045	0.6137
System Cost ($)	0.6416	0.6464
Battery remaining energy (pu)	0.7014	0.6974

Fig. 23 compares fuel cell power estimates obtained by DP to those obtained by

ANN over portion of the UDDS cycle. The fuel cell operated between 779 and 781 seconds

and between 80.3 and 805 seconds with DP. However, the fuel cell operated briefly with

ANN between 802 and 804 seconds showing that less fuel is being consumed and the

power demand is being supplied mainly from the battery over this portion. The fuel cell

remaining energy is maintained with both DP and ANN thus satisfying CD mode

conditions as shown in Fig. 24. Although less H_2 is being consumed with ANN, but this has

resulted in the violation of the fuel cell limits and battery SOC limits where the SOC went
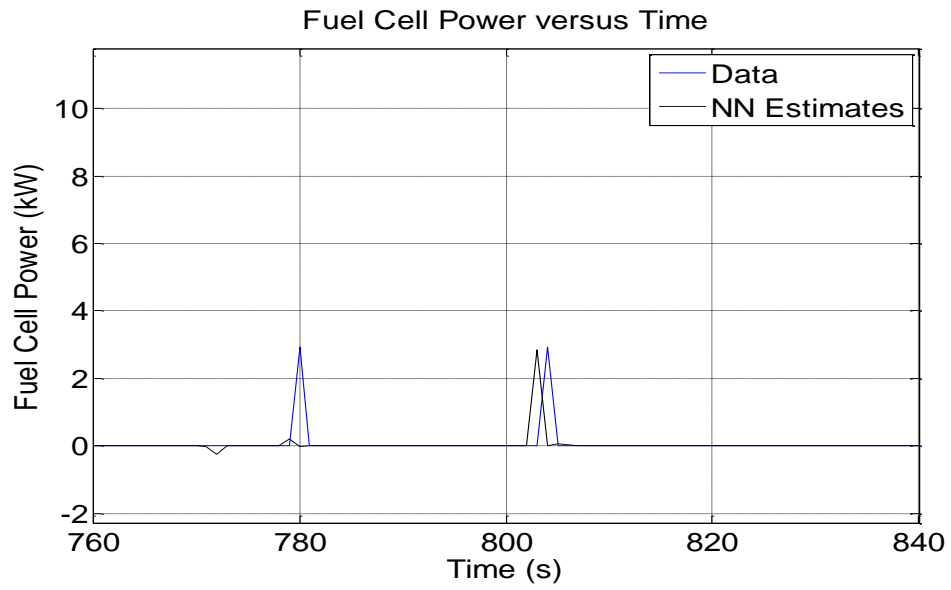
slightly below minimum.

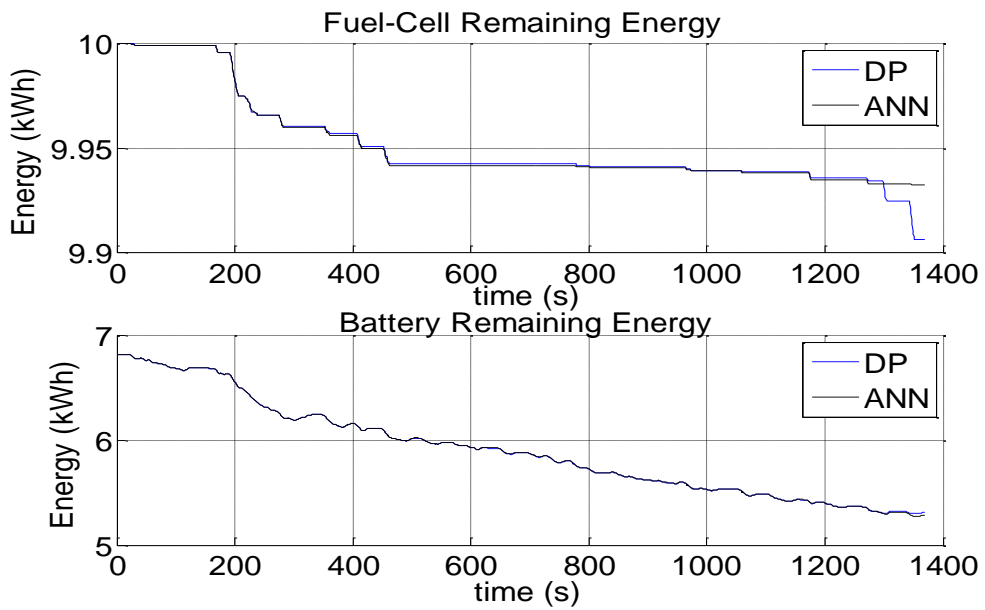Figure 23: The FC power estimates for ANN and DP over UDDS-CD

Figure 24: The FC and battery remaining energy for ANN and DP over UDDS-CD

After obtaining desired results, the generalization capabilities of the ANN are checked. The ANN is trained over the UDDS road and tested over the same drive cycle with a 10% faster and 10% slower variations.

As mentioned before that in addition to the speed, the time interval of the UDDS drive cycle is changed to maintain a constant distance in all cases. The results obtained show that the ANN works reasonably well when the speed of the UDDS cycle is changed as shown in Figs. 25 and 26 corresponding to faster and slower speeds respectively. In this case the ANN solution is also shifted from the DP but it is able to follow it at most of the periods. The battery remaining for CS operation is shown in Figs. 27 and 28 corresponding for faster and slower UDDS respectively. The SOC is slightly going below minimum by around 0.26% over faster UDDS and 0.08% over slower UDDS; therefore, there is no significant charge depletion or charge build-up. Table 9 shows a comparison between optimal results of DP and ANN results for faster and slower speeds, the system cost of ANN is close to that of DP as it has varied by around 2% for faster UDDS and 0.45% for slower UDDS.
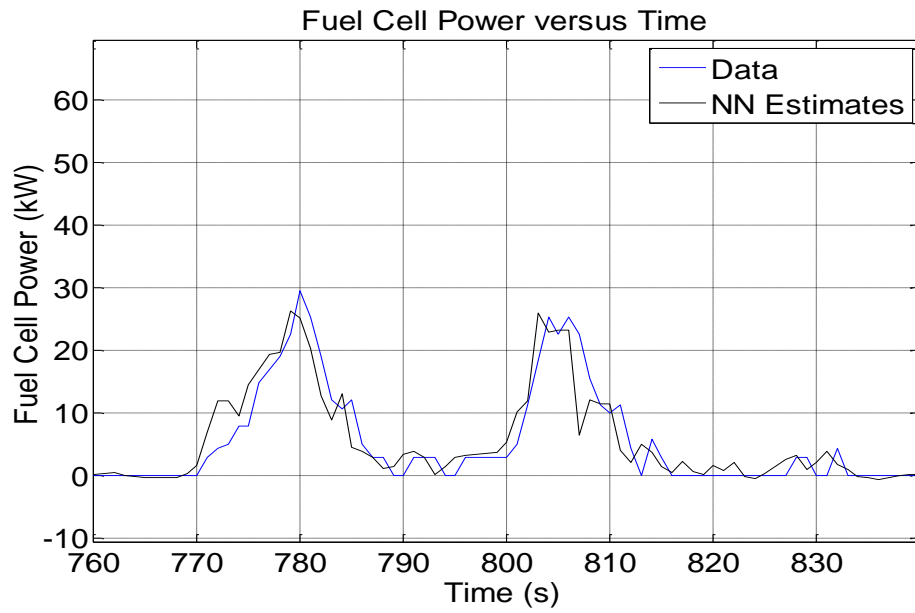
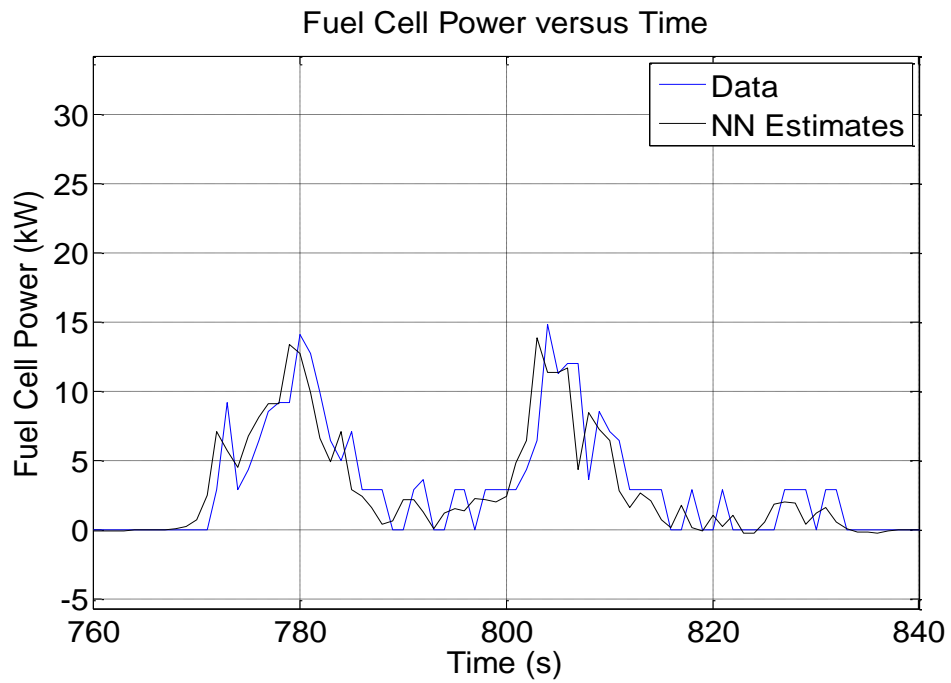Figure 25: The FC power estimates for ANN and DP over faster UDDS-CS

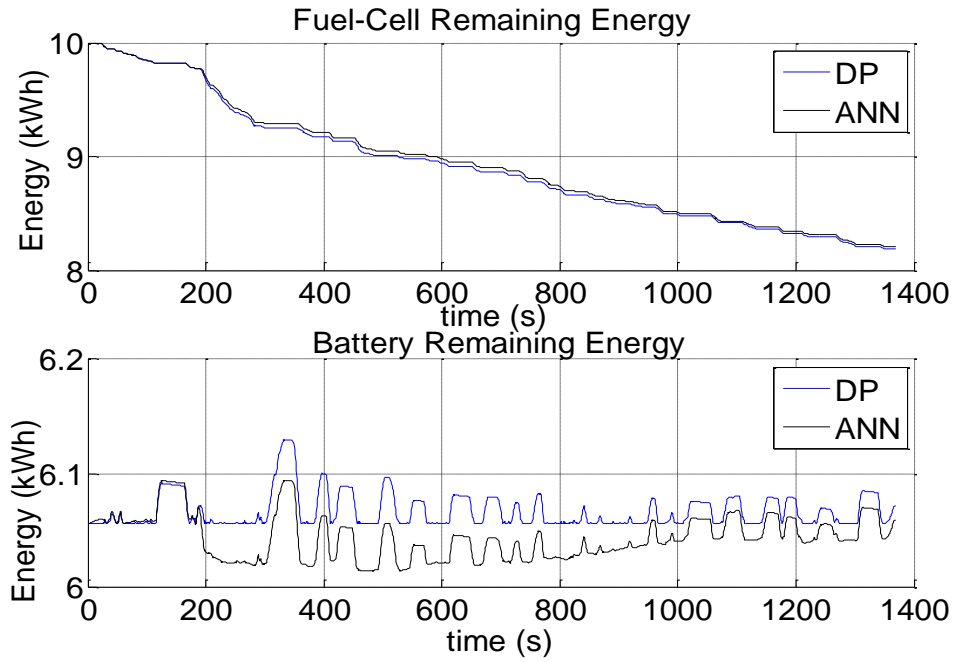Figure 26: The FC power estimates for ANN and DP over slower UDDS-CS

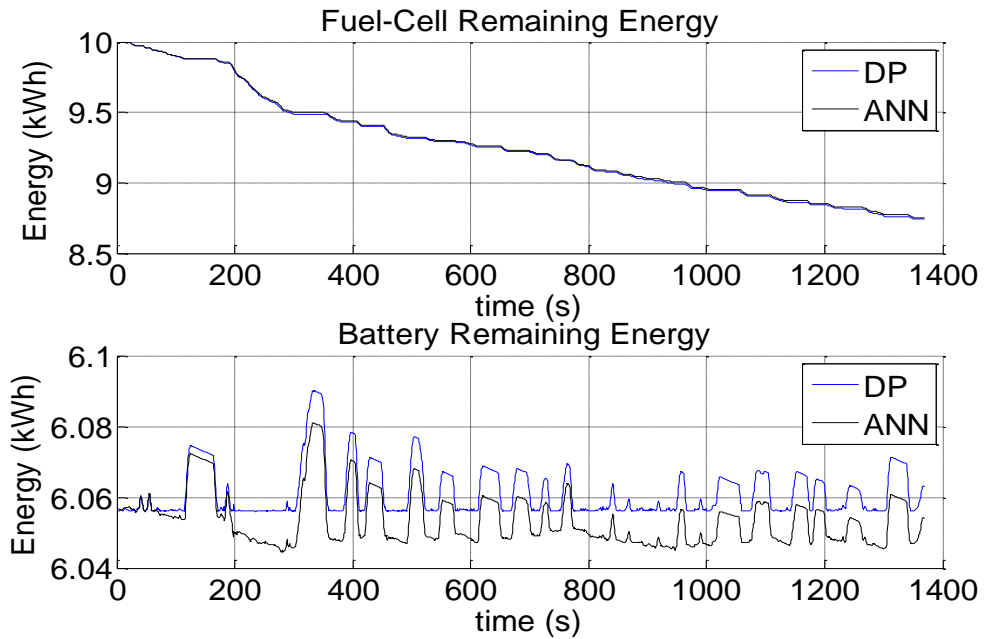Figure 27: The FC and battery remaining energy for ANN and DP over faster UDDS-CS

Figure 28: The FC and battery remaining energy for ANN and DP over slower UDDS-CS

Table 9: DP and ANN Results over Faster and Slower UDDS- CS Operation

Parameters	DP faster	ANN faster	DP slower	ANN slower
H$_2$ cost ($)	0.3212	0.3185	0.1845	0.1840
H$_2$ usage (g)	107.1	106.2	61.5	61.3
Battery Cost ($)	0.2172	0.2091	0.1049	0.1041
System Cost ($)	0.5383	0.5275	0.2894	0.2881
Battery Final SOC	0.8020	0.8006	0.8009	0.8009

Cross-generalization is also performed, where the ANN is trained over the UDDS drive cycle and tested over different drive cycles (i.e., HWFET and NEDC). The ANN is able to generalize fairly well in both cases. The fuel cell estimates are close to the fuel cell targets for HWFET and NEDC drive cycles as shown in Figs. 29 and 30 respectively where the solutions are also shifted but do not vary significantly. Concerning battery remaining energy, the DP and ANN results are close to each other for the HWFET with a small insignificant variation where the SOC goes below minimum by around 0.5% as shown in Fig. 31. However, for NEDC drive cycle the battery remaining energy shown in Fig. 32 goes below minimum with ANN by around 3.3% showing that better generalization is obtained with HWFET. Table 10 compares optimal results obtained by DP to the approximate ones obtained by ANN for both drive cycles showing again that ANN has better generalization capability over HWFET where the system cost increases by 1.2% as compared to DP; whereas it increases by around 5.5% over NEDC. This can be attributed to the shape of the HWFET road which is closer to UDDS road than NEDC.
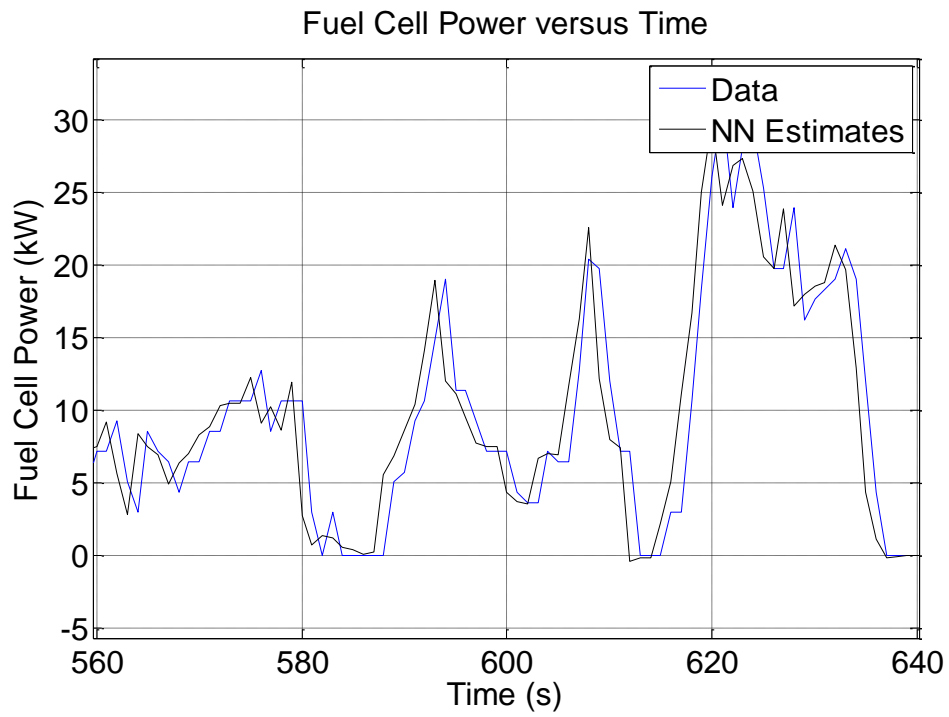
Figure 29: The FC power estimates for DP and ANN over HWFET-CS
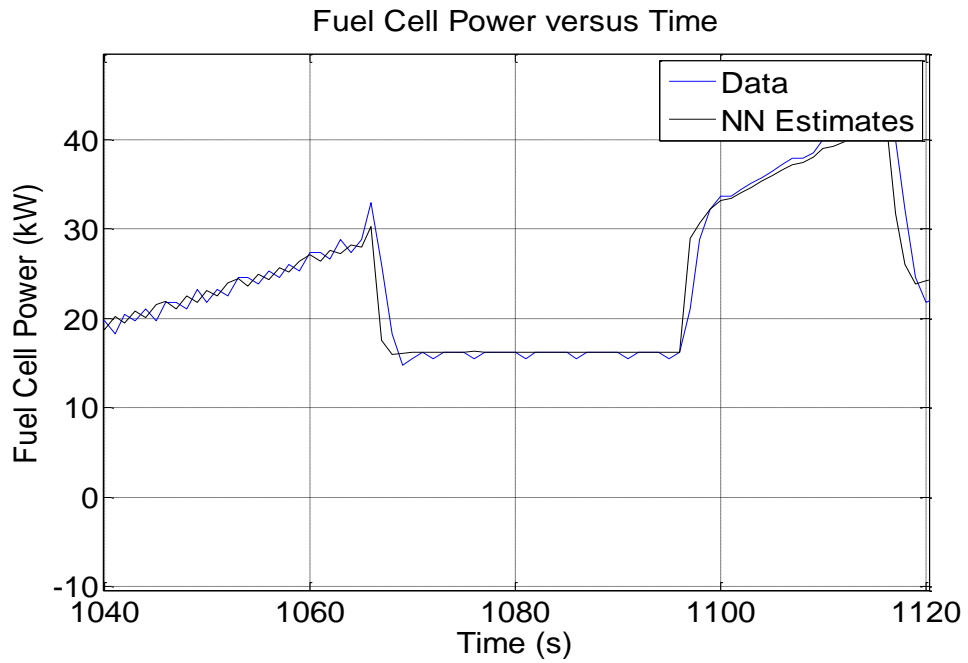

Figure 30: The FC power estimates for ANN and DP over NEDC-CS
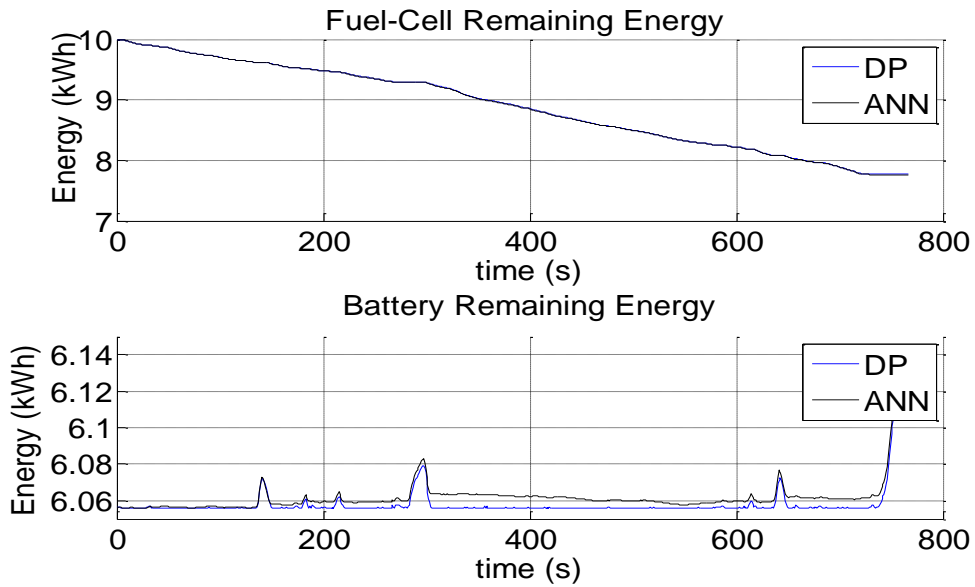
61

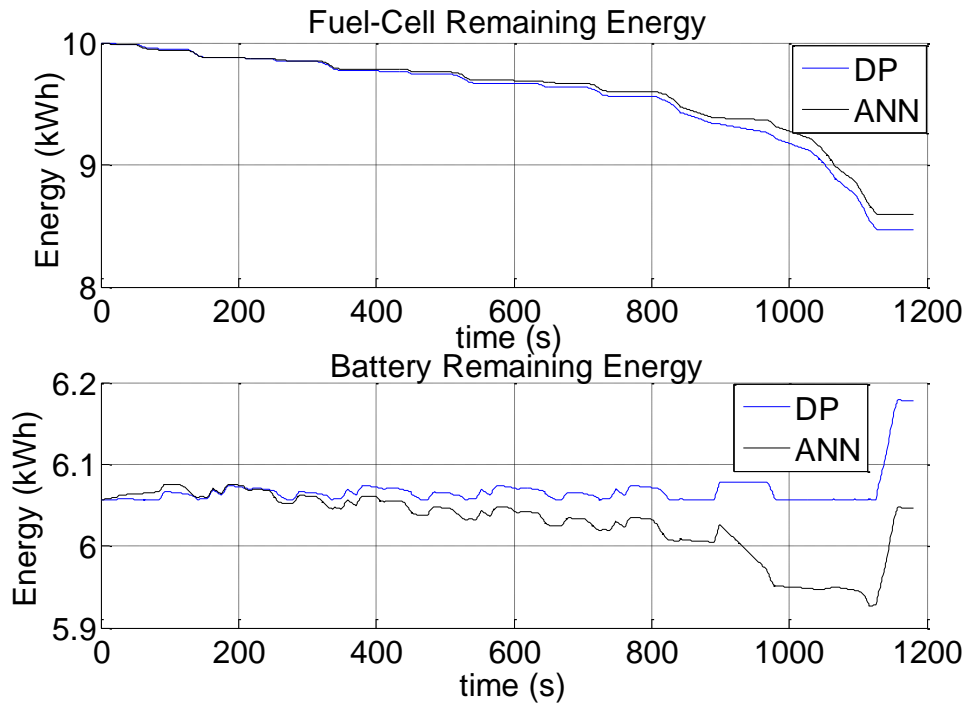Figure 31: The FC and battery remaining energy for ANN and DP over HWFET-CS

Figure 32: The FC and battery remaining energy for ANN and DP over NEDC-CS

Table 10: DP and ANN Results over HWFET and NEDC-CS

Parameters	DP HWFET	ANN HWFET	DP NEDC	ANN NEDC
H_2 cost ($)	0.3760	0.3797	0.2709	0.2477
H_2 Usage (g)	125.3	126.7	90.3	82.56
Battery Cost ($)	0.0339	0.0252	0.0621	0.1037
System cost ($)	0.4098	0.4049	0.3329	0.3514
Battery Final SOC	0.8082	0.8115	0.8160	0.7959

The ANN is able to produce results close to optimum ones when used in CS and CD mode. The SOC is not maintained like in the case of DP and SSDP since ANN cannot handle constraints, but the drift is small without significant charge build-up or charge depletion. The proposed ANN shows good generalization capability when tested over faster and slower UDDS and over new drive cycles.

C. Speed Forecast Results

As mentioned earlier, the models with high orders are better in terms of forecast (lower error), but when it comes to the implementation of the speed forecast with SSDP, the 1st order produces better fuel saving results since the net curve of the forecasted speed is only shifted from the actual speed by 1 step. Table 11 shows a comparison between the results of a SSDP model applied using speed forecasted by models of different orders. The results show that the persistence model when used with SSDP method produces results very close to SSDP model using the actual speed, where the system cost varies by around 0.51% compared to 19.5% with 2nd order model and 24% with 3rd and 4th order models. Figs. 33 and 34 show the results of forecasted speed compared to measured speed obtained by 4th

order and 1st order models without constant respectively. With the first order model the

forecasted speed is only shifted by one step from the actual speed as illustrated in Fig. 33,

and the model error of the 4th order is lower than that of the 1st order.

Table 11: Comparison between Different Speed Forecast Model Orders used with SSDP
over UDDS with SOC0 =0.8

| Forecast error & fuel economy	Actual speed	Forecast model Order 1	Forecast model Order 2	Forecast model Order 3	Forecast model Order 4
Forecast error		6.9819	1.3191	1.2685	1.2670
H_2 cost (\$)	0.2711	0.2701	0.2941	0.2994	0.299
Battery degradation (\$)	0.1770	0.1757	0.2413	0.2568	0.2568
System cost (\$)	0.4481	0.4458	0.5354	0.5562	0.5558
H_2 consumption (g)	90.4	90.04	98.0	99.8	99.7
Battery Remaining energy (pu)	0.8014	0.8014	0.8015	0.8015	0.8015
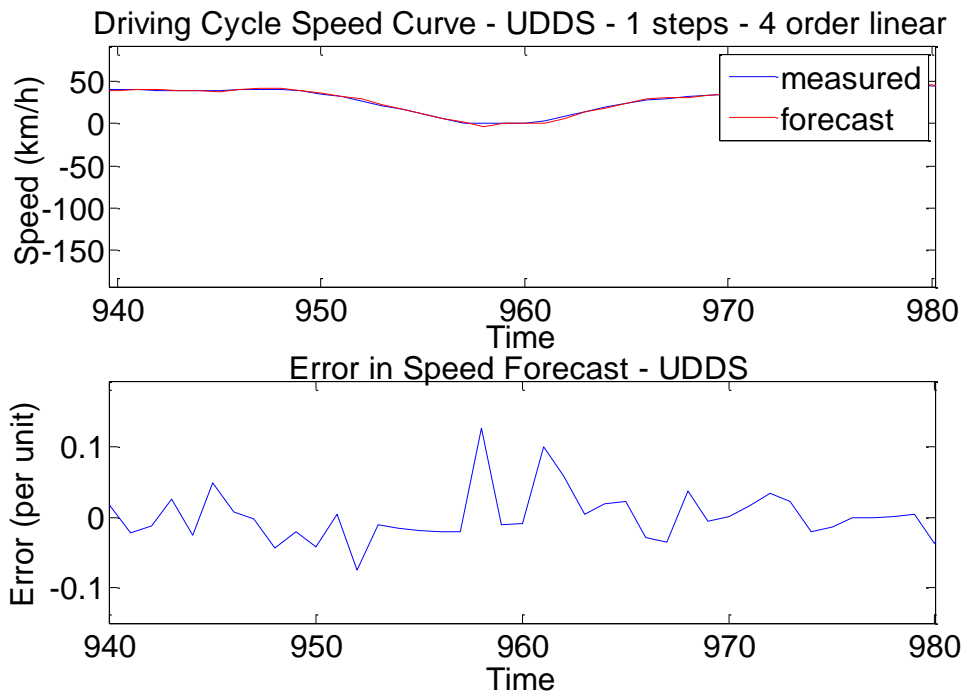
Figure 33: Measured speed compared to forecasted speed using 4th order model without constant
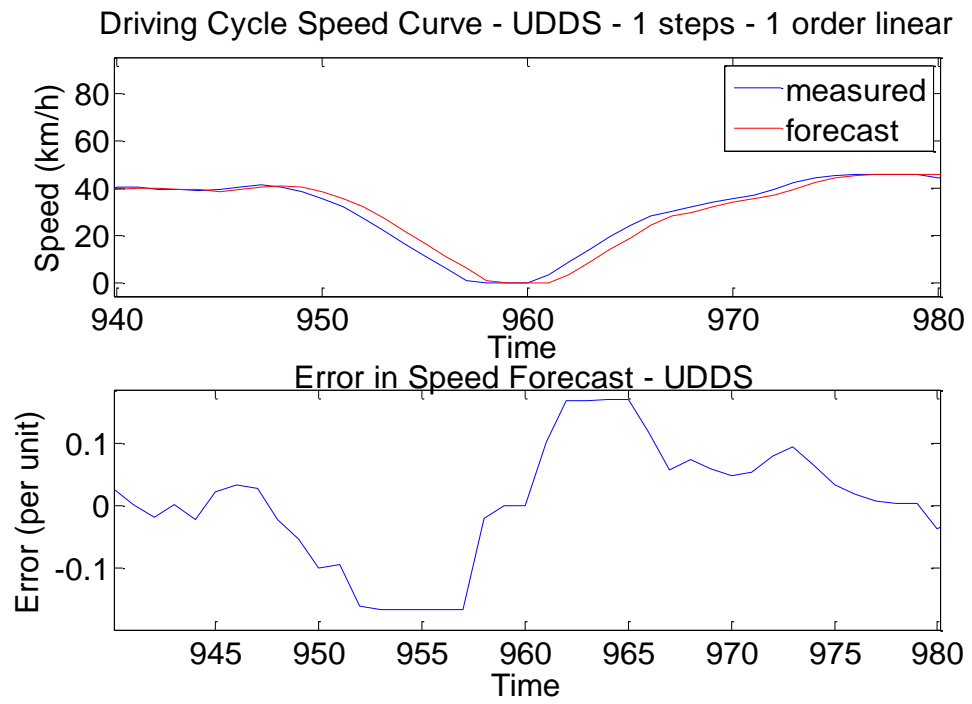
Figure 34: Measured speed compared to forecasted speed using 1st order model without constant

CHAPTER VI

CONCLUSION

This work has presented new energy management strategy for HEV known as single step dynamic programming (SSDP) technique, and a control strategy based on artificial neural network (ANN). These control strategies which are derived from dynamic programming (DP) can easily lend themselves for real time implementation. Global optimization techniques, on the other hand, such as DP evaluate the fuel economy of a given power train configuration producing optimum results. For this control law to be implementable the future driving conditions should be known; which is not the case in real time. However, the results of DP establish a benchmark for evaluating the optimality of the realizable control strategies. The SSDP optimization technique differs from DP in that it does not have back-tracing, and this might cause some infeasibility; however, the forward-looking models are more realistic than those that are backward looking. The infeasibility is SOC violation and it is very small without any fuel cell ramp rate violations. It is shown that the infeasibility and the system cost are affected by the chosen number of levels. The number of violations, the size of added penalty, and the system cost decrease as the number of levels increases until they reach a saturation value. SSDP has a lower computational load than DP, the performance in terms of fuel economy for both methods is practically very close, and the infeasibility in case of SSDP is physically not serious; therefore, it can be asserted that a very slightly sub-optimal solution can be achieved with a technique much simpler and more realistic than the one leading to the optimal policy. Moreover, SSDP is

faster than DP by around 86.84%, and therefore it can be used in system sizing which is advantageous because when the system is faster, more cases can be examined and the quality of the plans obtained will be improved [28]. The proposed ANN on the other hand is trained based on DP results carried out off-line. It can be implemented in real time as it takes one step at a time. It requires training and has no mechanism to control the SOC; there will always be a drift. However, ANN is able to produce results very close to optimum ones. It is also able to slightly maintain the battery remaining energy in the CS operation without significant charge build-up or charge depletion, even though at some periods the SOC is going slightly below minimum, and the final and initial SOC do not exactly match like in the case of DP or SSDP due to the suboptimal nature of ANN that is not able to handle constraints. Therefore, the proposed SSDP method is better than ANN in solving the power split problem since its results are closer to optimum ones, it can handle constraints better, it can maintain SOC in CS operation without the drift at the end of the drive cycle, and it does not require training. Both SSDP and ANN provide an easy mechanism to change from CS to CD modes of operation. To solve the SSDP and the ANN methods, the demand at the next step should be known a priori. This demand is obtained by applying a one step-ahead speed forecast. Models of different orders are tested, and their beta coefficients are examined for different drive cycles. Since only the constant β_0 changes as the speed of the drive cycle changes, β_0 is not included in the speed forecast model in order to have a more stable model. Moreover, the beta coefficients suitable for one drive cycle are not optimal for the other. Therefore, there is no choice of the parameters that can be performed only once as initialization of the control strategy and applied in every

situation, but it is found out that beta coefficients do not have significant effects on the results. Testing shows that higher order models are able to forecast the speed with a small error but the 1st order model known as the persistence forecast is able to produce better fuel saving results than higher order models when used with SSDP, since the net curve of the forecasted speed is only shifted by 1 step from the actual speed in this case. Therefore, the first order linear model is used. Also by using a first order speed forecast model there will be no need to do an adaptive mechanism that adapts to changes in road conditions since $\beta = 1$, and execution time in this case is not considered since the forecasted speed at time k is simply the actual speed at time $k - 1$.

BIBLIOGRAPHY

1. Pérez-Lombard, L., Ortiz, J., & Pout, C. (2008). A review on buildings energy consumption information. Energy and buildings, 40 (3), 394-398.

2. Karaki, S. H., Jabr, R., Chedid, R., & Panik, F. (2015). Optimal Energy Management of Hybrid Fuel Cell Electric Vehicles (No. 2015-01-1359). SAE Technical Paper.

3. Schell A., Peng H., Tran D., Stamos E., Lin C. C., Kim M. J. (2005). Modeling and control strategy development for fuel cell electric vehicles, *Annual Reviews in Control*, 29, 159–168.

4. Perez L. V., Pilotta E. A. (2009). Optimal power split in a hybrid electric vehicle using direct transcription of an optimal control problem, *Mathematics and Computers in Simulation*, 79, 1959–70.

5. Boyali, A. and L. Guvenc (2010). "Real-time controller design for a parallel hybrid electric vehicle using neuro-dynamic programming method", 2010 IEEE International Conference on Systems Man and Cybernetics (SMC), pp. 4318 – 4324.

6. Feldkamp, L., Abou-Nasr, M., & Kolmanovsky, I. V. (2009, March). Recurrent neural network training for energy management of a mild hybrid electric vehicle with an ultra-capacitor. In Computational Intelligence in Vehicles and Vehicular Systems, 2009. CIVVS'09. IEEE Workshop on (pp. 29-36). IEEE.

7. Yi, T., Xin, Z., Liang, Z., & Xinn, Z. (2009, December). Intelligent energy management based on driving cycle identification using fuzzy neural network. In Computational Intelligence and Design, 2009. ISCID'09. Second International Symposium on (Vol. 2, pp. 501-504). IEEE.

8. Lin W. S. , Zheng C. H. (2011). Energy management of a fuel cell/ultra-capacitor hybrid power system using an adaptive optimal-control method, Journal of Power Sources, 196, 3280–3289.

9. Quigley, C. P., Ball, R. J., Vinsome, A. M., & Jones, R. P. (1996, September). Predicting journey parameters for the intelligent control of a hybrid electric vehicle. In Intelligent Control, 1996. Proceedings of the 1996 IEEE International Symposium on (pp. 402-407). IEEE.

10. Xiong W., Zhang Y., Yin C. (2009). Optimal energy management for a series-parallel hybrid electric bus, Energy Conversion and Management, 50, 1730–1738.

11. Erdinc O., Vural B., Uzunoglu M. (2009). A wavelet-fuzzy logic based energy management strategy for a fuel cell/battery/ultra-capacitor hybrid vehicular power system, Journal of Power Sources, 194, 369–380.

12. Kim, N., & Rousseau, A. P. (2011). Comparison between rule-based and instantaneous optimization for a single-mode, power-split HEV (No. 2011-01-0873). SAE Technical Paper.

13. Ambuhl D., Sundstrom O., Sciarretta A., Guzzella L. (2010). Explicit optimal control policy and its practical application for hybrid electric power-trains, *Control Engineering Practice*, 18, 1429–1439.

14. Sorrentino M., Rizzo G., Arsie I. (2011). Analysis of a rule-based control strategy for on-board energy management of series hybrid vehicles, *Control Engineering Practice*, 19, 1433–1441.

15. Panik F., Huang Y., Boff A., Gonzalves S., Battista E. (2011). Design and Simulation Models for a Brazilian Hybrid Delivery Truck, *SAE International*, Paper No. 2011-36-0162.

16. Musardo, C., Rizzoni, G., Guezennec, Y., & Staccia, B. (2005). A-ECMS: An adaptive algorithm for hybrid electric vehicle energy management. European Journal of Control, 11(4), 509-524.

17. Onori, S., Serrao, L., & Rizzoni, G. (2010, January). Adaptive equivalent consumption minimization strategy for hybrid electric vehicles. In ASME 2010 Dynamic Systems and Control Conference (pp. 499-505). American Society of Mechanical Engineers.

18. Sciarretta, A., Back, M., & Guzzella, L. (2004). Optimal control of parallel hybrid electric vehicles. Control Systems Technology, IEEE Transactions on,12(3), 352-363.

19. Rousseau, G., Sinoquet, D., Sciarretta, A., & Milhau, Y. (2011). Design optimization and optimal control for hybrid vehicles. Optimization and Engineering, 12(1-2), 199-213.

20. Gurkaynak, Y., Khaligh, A., & Emadi, A. (2010, September). Neural adaptive control strategy for hybrid electric vehicles with parallel powertrain. In Vehicle Power and Propulsion Conference (VPPC), 2010 IEEE (pp. 1-6). IEEE.

21. Bernard J., Delprat S., Guerra T.M., Buchi F.N. (2010). Fuel efficient power management strategy for fuel cell hybrid power-trains, Control Engineering Practice, 18, 408–417.

22. Serrao L., A. Sciarretta, O. Grondin, A. Chasse, Y. Creff, Domenico di Domenico, P. Pognant-Gros, C. Querel and L. Thibault (2011). "Open Issues in Supervisory

Control of Hybrid Electric Vehicles: A Unified Approach using Optimal Control Methods", Int. Scientific Conf. on hybrid and electric vehicles (RHEVE 2011), 6-7 December 2011.

23. Dinnawi, R., Fares, D., Chedid, R., Karaki, S., & Jabr, R. (2014, April). Optimized energy management system for fuel cell hybrid vehicles. In Mediterranean Electro technical Conference (MELECON), 2014 17th IEEE (pp. 97-102). IEEE.

24. Wang, R., & Lukic, S. M. (2012, March). Dynamic programming technique in hybrid electric vehicle optimization. In Electric Vehicle Conference (IEVC), 2012 IEEE International (pp. 1-8). IEEE.

25. Johannesson L., Pettersson S., Egardt B. (2009). Predictive energy management of a 4QT series-parallel hybrid electric bus, Control Engineering Practice, 17, 1440–1453.

26. Rizzoni G., Guzzella L., and Baumann B. M. (1999). United modeling of hybrid electric vehicle drivetrains", IEEE/ASME Transactions on Mechatronics, vol. 4, no. 3, pp. 246-257.

27. Qi, Y., & Ishak, S. (2013). Stochastic approach for short-term freeway traffic prediction during peak periods. Intelligent Transportation Systems, IEEE Transactions on, 14(2), 660-672.

28. Karaki, S. H., Dinnawi, R., Jabr, R., Chedid, R., & Panik, F. (2015). Fuel Cell Hybrid Electric Vehicle Sizing using Ordinal Optimization. SAE International Journal of Passenger Cars-Electronic and Electrical Systems, 8(2015-01-0155), 60-69.